Model for a phase-space selector using microwave transitions

L. O. Castaños[1,2,*] and E. Gomez[2,†]

[1]*Departamento de Física Matemática, Instituto de Investigaciones en Matemáticas Aplicadas y en Sistemas, Universidad Nacional Autónoma de México, C.P. 04510, Mexico*

[2]*Instituto de Física, Universidad Autónoma de San Luis Potosí, San Luis Potosí 78290, Mexico*

(Received 6 September 2013; revised manuscript received 24 November 2013; published 13 January 2014)

We establish a model to describe any alkali-metal atom interacting with a position- and time-dependent magnetic field. It includes the hyperfine structure of the atom and quantizes its center-of-mass motion. The model is used to characterize a proposed phase-space selector. It consists of a method based on hyperfine magnetic dipole transitions to prepare samples of atoms with well-defined position and velocity. The evolution of the atom is determined analytically and relevant physical quantities such as the probability of transition and the expected values of position and momentum are analyzed. It is concluded that the phase-space selector can lead to samples of atoms whose width in velocity tends to those obtained using velocity-dependent Raman transitions.

DOI: 10.1103/PhysRevA.89.013406 PACS number(s): 32.60.+i, 03.75.Be, 03.75.Dg, 03.65.Nk

I. INTRODUCTION

Raman transitions between two hyperfine sublevels are an important tool used in experimental physics to manipulate alkali-metal atoms [1–12]. They involve the simultaneous absorption and stimulated emission by an atom and can be implemented in a copropagating or counterpropagating laser beam configurations. In the latter, Doppler shifts add and the Raman transition becomes sensitive to the velocity of the atoms. These velocity-dependent Raman transitions can be used to prepare samples of atoms with well-defined velocity [1–3] which, in turn, can be used, for example, to make matter-wave interferometers [4] and to measure forces [5–7] and fundamental constants [8,9]. Moreover, Raman transitions have found applications in diverse fields such as dynamics in optical lattices [10], quantum decoherence, and chaos [11,12]. Therefore, developing other methods that can be used to prepare samples of atoms with well-defined position or velocity and that exhibit other virtues when compared to Raman transitions is important. In this article we propose one method based on hyperfine magnetic dipole transitions. We now present the ideas behind it.

We first describe how one can select in position, that is, how one can obtain a sample of atoms with well-defined position. Consider a cloud of noninteracting alkali-metal atoms in a static magnetic field $\mathbf{B}(\mathbf{r})$ that depends on position and prepare all the atoms in one of the ground-state hyperfine sublevels, say $|1\rangle$. Among all the atoms in the cloud one wishes to select only those in a small neighborhood $V(\mathbf{r}_0)$ around a fixed position $\mathbf{r}_0$. One can do this by sending only the atoms in $V(\mathbf{r}_0)$ to another of the ground-state hyperfine sublevels, say $|2\rangle$, and then applying a laser field that gets rid of the atoms outside $V(\mathbf{r}_0)$, that is, that pushes away the atoms that remained in state $|1\rangle$. This can be done by noticing that, as a result of the Zeeman effect and the dependence on position of $\mathbf{B}(\mathbf{r})$, states $|1\rangle$ and $|2\rangle$ have an energy difference $\Delta E(\mathbf{r})$ that depends on the position $\mathbf{r}$ in which each atom is located. Only the atoms in $V(\mathbf{r}_0)$ have $\Delta E(\mathbf{r}) \simeq \Delta E(\mathbf{r}_0)$. Hence, one can apply a π pulse using a monochromatic magnetic field $\mathbf{B}_p(\mathbf{r},t)$ that is quasiresonant with the $|1\rangle \leftrightarrow |2\rangle$ transition for atoms inside $V(\mathbf{r}_0)$. The π pulse will send all the atoms in $V(\mathbf{r}_0)$ to state $|2\rangle$, while all the atoms outside $V(\mathbf{r}_0)$ will remain in state $|1\rangle$ because they are far off resonance. In this way one obtains a sample of atoms in a small neighborhood $V(\mathbf{r}_0)$ of $\mathbf{r}_0$; that is, one selected atoms in position.

The selection in velocity is achieved by selecting in position at two different times. After the first selection in position, assume that the sample of atoms in state $|2\rangle$ and in a small neighborhood $V(\mathbf{r}_0)$ of $\mathbf{r}_0$ starts moving vertically (for example, the atoms move due to gravity or a laser field pushes the atoms). At a certain instant make another selection in position; that is, apply a π pulse using a monochromatic magnetic field $\mathbf{B}_p(\mathbf{r},t)$ that is quasiresonant with the $|1\rangle \leftrightarrow |2\rangle$ transition for atoms inside a small neighborhood $V(\mathbf{r}_1)$ around $\mathbf{r}_1$. As a consequence of the two selections in position a selection in velocity has been performed; that is, the cloud of atoms in state $|1\rangle$ [the atoms in $V(\mathbf{r}_1)$] has well-defined velocity. One can get rid of the atoms in state $|2\rangle$ by applying a laser field that pushes them away. Moreover, the cloud of atoms in state $|1\rangle$ will become spatially separated from the cloud of atoms in state $|2\rangle$ because the clouds move under different potentials due to the different response to the magnetic field of the two levels.

It is the purpose of this article to characterize the phase-space selector described above, that is, the selections in position and in velocity described above. In order to do this we introduce a model that describes an alkali-metal atom interacting with a classical magnetic field and establish its regime of validity. The model includes the hyperfine structure of the atom and quantizes the center-of-mass motion.

The article is organized as follows. In Sec. II we review the internal structure of an alkali-metal atom. In Sec. III we introduce the model that describes an alkali-metal atom with quantized center-of-mass motion and interacting with a classical magnetic field. In Secs. IV and V we investigate the evolution of the atom before and during the application of $\mathbf{B}_p(\mathbf{r},t)$. In Sec. VI we characterize the selections in position and in velocity. Finally, the conclusions are given in Sec. VII.

*LOCCJ@yahoo.com

†egomez@ifisica.uaslp.mx

II. INTERNAL STRUCTURE OF AN ALKALI-METAL ATOM

In this section we briefly review the internal structure of an alkali-metal atom in the mean-field approximation. All the details are provided in Appendix A.

The ground-state configuration of an alkali-metal atom consists of a series of full shells followed by a single s electron. Moreover, the internal configuration is so stable that all except high excited states of the atom involve only the valence electron. Hence, to good approximation alkali-metal atoms can be treated by a model in which a single electron moves in a spherically symmetric non-Coulomb potential. In this mean-field approximation the Hamiltonian of an alkali-metal atom of mass M in the ground-state configuration and whose nucleus is fixed at a position is given by [13–15]

$$H_A = \frac{a}{\hbar^2}\mathbf{I}\cdot\mathbf{J} + \frac{\hbar\Delta W}{2(2I+1)}. \tag{1}$$

Here $a = 2\hbar\Delta W/(2I+1)$, $\hbar\Delta W$ is the field-free ground-state (energy) hyperfine splitting, $\mathbf{I}$ is the nuclear spin angular momentum operator, I is the nuclear spin, and $\mathbf{J}$ is the total angular momentum operator of the valence electron (the sum of the orbital plus the spin angular momentum operators). In the rest of the article we assume that $I \geqslant 1/2$.

We emphasize that we are restricting to the ground-state configuration of the atom, that is, we have restricted the principal quantum number n to its smallest value n_0 and we have taken the azimuthal quantum number l to be zero. Hence, $\mathbf{J} = \mathbf{S}$ with $\mathbf{S}$ the spin angular momentum operator of the valence electron and the state space $\mathcal{H}_0$ of the alkali-metal atom is spanned by the orthonormal basis

$$\begin{aligned}\beta_0 = \{&|k_0,m_s,m_I\rangle \equiv |k_0\rangle\otimes|s=1/2,m_s\rangle\otimes|I,m_I\rangle :\\ &m_s = \pm 1/2,\quad m_I = I, I-1,\ldots,-I\}.\end{aligned} \tag{2}$$

Here $|k_0\rangle \equiv |n=n_0,l=0,m_l=0\rangle$. The basis β_0 is composed of eigenvectors of $\mathbf{S}^2$, S_z, $\mathbf{I}^2$, and I_z.

Introducing the total angular momentum operator of the atom $\mathbf{F} = \mathbf{J}+\mathbf{I}$, one can define another orthonormal basis β_0^{C} for $\mathcal{H}_0$ composed of eigenvectors of H_A, $\mathbf{S}^2$, $\mathbf{I}^2$, $\mathbf{F}^2$, and F_z,

$$\begin{aligned}\beta_0^{\mathrm{C}} = \{&|k_0,F,M_F\rangle \equiv |k_0\rangle\otimes|F,M_F\rangle :\\ &-F\leqslant M_F\leqslant F,\quad F = F_\pm\},\end{aligned} \tag{3}$$

with

$$F_\pm \equiv I \pm \tfrac{1}{2}. \tag{4}$$

For each $-F\leqslant M_F\leqslant F$ and $F = F_\pm$, one has

$$H_A|k_0,F=F_\pm,M_F\rangle = \pm\frac{\hbar\Delta W}{2}|k_0,F=F_\pm,M_F\rangle. \tag{5}$$

We now introduce a constant classical magnetic field along the z axis, $\mathbf{B} = B\mathbf{z}$, with $B\in\mathbb{R}$. The Hamiltonian of the system atom + magnetic field is [13–15]

$$H_{\mathrm{AB}} = H_A - \boldsymbol{\mu}\cdot\mathbf{B}, \tag{6}$$

where $\boldsymbol{\mu}$ is the magnetic moment operator of the atom and is given by

$$\boldsymbol{\mu} = -g_l\frac{\mu_B}{\hbar}\mathbf{L} - g_s\frac{\mu_B}{\hbar}\mathbf{S} + g_I\frac{\mu_N}{\hbar}\mathbf{I}. \tag{7}$$

The summands on the right of (7) are, respectively, the orbital and spin magnetic moment operators of the valence electron and the nuclear magnetic moment operator. Moreover, g_l and g_s are the electron orbital and spin g factors, while g_I is the nuclear g factor. Also, $\mu_B = \hbar e/(2m_e)$ is the Bohr magneton and $\mu_N = \hbar e/(2m_p)$ is the nuclear magneton with $e>0$ the elementary charge and m_e and m_p the mass of the electron and the proton, respectively. We mention that one must be careful when one compares expression (7) with other references, since some take the nuclear g factor as $-g_I m_e/m_p$ instead of g_I (for example, compare [14,16,17]). Nevertheless, the results can be rewritten in terms of one convention or the other. Note that the state space of the system is still $\mathcal{H}_0$.

To diagonalize H_{AB} first define

$$x = \frac{B}{\Delta W}\left(g_s\frac{\mu_B}{\hbar} + g_I\frac{\mu_N}{\hbar}\right),\quad \gamma_1 = \frac{g_s - 2Ig_I\frac{m_e}{m_p}}{2\left(g_s + g_I\frac{m_e}{m_p}\right)},$$

$$\gamma_2 = \frac{g_I\frac{m_e}{m_p}}{g_s + g_I\frac{m_e}{m_p}},$$

$$\theta(M_F,x) = \tan^{-1}\left[\frac{\sqrt{1-\left(\frac{M_F}{F_+}\right)^2}}{\left(\frac{M_F}{F_+}\right)+x}\right]\in[0,\pi),$$

$$V_{F_+,\pm F_+}(x) = \frac{\hbar\Delta W}{2}(1\pm 2\gamma_1 x),$$

$$V_{F_\pm,M_F}(x) = \frac{\hbar\Delta W}{2}\left(-2M_F\gamma_2 x \pm\sqrt{1+2\frac{M_F}{F_+}x+x^2}\right),$$

$$|V_{F_+,\pm F_+}(x)\rangle = \left|k_0,m_s=\pm\frac{1}{2},m_I=\pm F_+\mp\frac{1}{2}\right\rangle,$$

and

$$\begin{aligned}&|V_{F_\pm,M_F}(x)\rangle\\ &\quad= \cos\left[\frac{\theta(M_F,x)}{2}\right]\left|k_0,m_s=\pm\frac{1}{2},m_I=M_F\mp\frac{1}{2}\right\rangle\\ &\qquad\pm\sin\left[\frac{\theta(M_F,x)}{2}\right]\left|k_0,m_s=\mp\frac{1}{2},m_I=M_F\pm\frac{1}{2}\right\rangle,\end{aligned} \tag{8}$$

for each $M_F = F_-,F_--1,\ldots,-F_-$. Since $B\in\mathbb{R}$, x is a nondimensional quantity that can be positive or negative. Before proceeding we make some comments on the notation chosen. We write $|V_j(x)\rangle$ and $V_j(x)$ with $j = F,M_F$ because these quantities depend on x and j and the latter will be potentials that affect the motion of the atom when the center-of-mass motion is quantized. Moreover, the $|V_j(x)\rangle$ reduce to eigenvectors of $\mathbf{F}^2$ and F_z with respective eigenvalues $F(F+1)\hbar^2$ and $M_F\hbar$ when $B=0$. Finally, the $|V_j(x)\rangle$ play the role of the kets $|1\rangle$ and $|2\rangle$ in the Introduction, while $V_j(x)-V_{j'}(x)$ play the role of the energy difference $\Delta E(\mathbf{r})$.

It follows that

$$\Gamma(x) = \left\{\left|V_{F,M_F}(x)\right\rangle : -F\leqslant M_F\leqslant F, F=F_\pm\right\} \tag{9}$$

is an orthonormal basis for $\mathcal{H}_0$ composed of eigenvectors of H_{AB}, since

$$H_{\mathrm{AB}}\left|V_{F,M_F}(x)\right\rangle = V_{F,M_F}(x)\left|V_{F,M_F}(x)\right\rangle, \tag{10}$$

for each $-F \leqslant M_F \leqslant F$, $F = F_\pm$. The formulas for the eigenvalues of $H_{\rm AB}$ are known in the literature as the *Breit-Rabi formula* [15,18].

III. AN ALKALI-METAL ATOM INTERACTING WITH A MAGNETIC FIELD

Consider an alkali-metal atom with quantized center-of-mass motion along the z axis, subject to a constant gravitational field, and interacting with a classical magnetic field of the form $B_{\rm ST}(z)\mathbf{z} + \mathbf{B}_p(t)$ with $\mathbf{z}$ the unit vector in the direction of the positive z axis. Appendix B gives an example of how a magnetic field of the form $B_{\rm ST}(z)\mathbf{z}$ can be produced.

The Hamiltonian of the system in the long-wavelength approximation and neglecting terms of order m_e/M is

$$H(t) = \frac{1}{2M}P_z^2 + Mg_0Z + H_A - \boldsymbol{\mu}\cdot[B_{\rm ST}(Z)\mathbf{z} + \mathbf{B}_p(t)]. \tag{11}$$

Here M is the mass of the atom, Z and P_z are the center-of-mass position and momentum operators along the z axis, respectively, $g_0 = 9.8\ \mathrm{m/s^2}$ is the acceleration of gravity, $\boldsymbol{\mu}$ is the magnetic dipole moment operator of the atom given in (7), and H_A is the Hamiltonian in (1). Appendix C shows how the Hamiltonian of an alkali-metal atom with center-of-mass motion quantized in three dimensions can be reduced to (11).

We take $\mathbf{B}_p(t)$ to be a monochromatic plane wave propagating in the direction of the positive x axis with polarization $\mathbf{b}_p$ and with (angular) frequency ω_A. Moreover, $t_0 \geqslant 0$ is the instant in which $\mathbf{B}_p(t)$ is turned on, while $t_1 > t_0$ is the instant in which it is turned off. Explicitly,

$$\mathbf{B}_p(t) = \mathbf{b}_p B_0(t)[e^{i\omega_A(t-t_0)} + e^{-i\omega_A(t-t_0)}]. \tag{12}$$

Here $\mathbf{b}_p$ is a constant unit real vector perpendicular to the x axis,

$$B_0(t) = \begin{cases} \frac{B_0}{2} & \text{if} \quad t_0 < t < t_1, \\ 0 & \text{if} \quad t \leqslant t_0 \quad \text{or} \quad t \geqslant t_1, \end{cases} \tag{13}$$

and $B_0 > 0$. The intention here is to use $B_{\rm ST}(z)\mathbf{z}$ to produce position-dependent internal energy shifts in the atom by the Zeeman effect, while $\mathbf{B}_p(t)$ is used to manipulate the internal state of the atom.

The state space of the system is

$$\mathcal{H}_{\rm CM} \otimes \mathcal{H}_0; \tag{14}$$

that is, we consider only the ground-state configuration of the atom. The state of the system at time t will be denoted by $|\psi(t)\rangle$.

Two orthonormal bases for $\mathcal{H}_0$ are β_0 and $\beta_0^{\rm C}$ given, respectively, in (2) and (3). According to (5), the latter is composed of eigenvectors of H_A. Moreover, two orthonormal bases (in the sense of Dirac) for $\mathcal{H}_{\rm CM}$ are the position and momentum bases:

$$\{|z\rangle : z \in \mathbb{R}\}, \quad \{|p\rangle : p \in \mathbb{R}\}. \tag{15}$$

Recall that $(H_A - \boldsymbol{\mu}\cdot B\mathbf{z})$ was diagonalized in Sec. II and the orthonormal basis $\Gamma(x)$ given in (8) and (9) was obtained. Replacing B with $B_{\rm ST}(z)$ and x with

$$x(z) = \left(g_s\frac{\mu_B}{\hbar} + g_I\frac{\mu_N}{\hbar}\right)\frac{B_{\rm ST}(z)}{\Delta W}, \tag{16}$$

one obtains an orthonormal basis

$$\Gamma[x(z)] = \left\{\left|V_{F,M_F}[x(z)]\right\rangle : \ (F,M_F) \in \mathcal{I}\right\}, \tag{17}$$

for $\mathcal{H}_0$ such that

$$\begin{aligned}&[H_A - \boldsymbol{\mu}\cdot B_{\rm ST}(z)\mathbf{z}]\left|V_{F,M_F}[x(z)]\right\rangle \\ &\quad = V_{F,M_F}[x(z)]\left|V_{F,M_F}[x(z)]\right\rangle.\end{aligned} \tag{18}$$

In order to introduce matrix representations, we assume the following ordering for $\mathcal{I}$:

$$\begin{aligned}\mathcal{I} = \{&(F_+,F_+),\ (F_+,-F_+),\ (F_+,F_-),\ (F_-,F_-),\\ &(F_+,F_- - 1),\ (F_-,F_- - 1),\ \ldots,\\ &(F_+,-F_-),\ (F_-,-F_-)\}.\end{aligned} \tag{19}$$

From now on we also use the more succinct notation $V_j[x(z)]$ with j an ordered pair $(F,M_F) \in \mathcal{I}$ instead of $V_{F,M_F}[x(z)]$.

Using bases (15) and (17) we obtain an orthonormal basis for $\mathcal{H}_{\rm CM} \otimes \mathcal{H}_0$,

$$\begin{aligned}\Gamma &= \{|z, V_j[x(z)]\rangle \\ &\equiv |z\rangle \otimes |V_j[x(z)]\rangle : z \in \mathbb{R},\ j \in \mathcal{I}\}.\end{aligned} \tag{20}$$

Notice that we have the following closure and orthonormalization relations

$$\mathbb{I} = \int_{-\infty}^{+\infty} dz \sum_{j\in\mathcal{I}} |z, V_j[x(z)]\rangle\langle z, V_j[x(z)]|,$$

and

$$\langle z, V_j[x(z)]|z', V_k[x(z')]\rangle = \delta(z - z')\delta_{jk}. \tag{21}$$

Here $\mathbb{I}$ is the identity operator in $\mathcal{H}_{\rm CM} \otimes \mathcal{H}_0$.

We now use the basis in (20) to express the Hamiltonian (11) as a matrix and Schrödinger's equation as a vector partial differential equation. In order to do this, first define the quantities

$$\begin{aligned}\psi_j(z,t) &= \langle z, V_j[x(z)]|\psi(t)\rangle, \\ \hbar\delta_j[x(z),t] &= \langle V_j[x(z)]|[-\boldsymbol{\mu}\cdot\mathbf{B}_p(t)]|V_j[x(z)]\rangle, \\ \hbar g_{jk}[x(z),t] &= (1-\delta_{jk})\langle V_j[x(z)]|[-\boldsymbol{\mu}\cdot\mathbf{B}_p(t)]|V_k[x(z)]\rangle,\end{aligned}$$

and

$$\begin{aligned}\mathcal{L}_{jk}(z) = \sum_{F=F_\pm}\sum_{M_F=-F}^{F}&\left(-\frac{\hbar^2}{2M}\right)\langle V_j[x(z)]|k_0,F,M_F\rangle \\ &\times\left\{\left[\frac{\partial^2}{\partial z^2}\langle k_0,F,M_F|V_k[x(z)]\rangle\right]\right. \\ &\left.+2\left[\frac{\partial}{\partial z}\langle k_0,F,M_F|V_k[x(z)]\rangle\right]\frac{\partial}{\partial z}\right\},\end{aligned} \tag{22}$$

where $j,k \in \mathcal{I}$. Notice that the diagonal matrix elements of $-\boldsymbol{\mu}\cdot\mathbf{B}_p(t)$ are given in $\hbar\delta_j[x(z),t]$, while its nondiagonal elements are included in $\hbar g_{jk}[x(z),t]$. Moreover, the terms $\mathcal{L}_{jk}(z)$ arise from the dependence on position of the basis $\Gamma[x(z)]$.

Now use (21) and (22) to express the state of the system $|\psi(t)\rangle$ as follows:

$$|\psi(t)\rangle = \int_{-\infty}^{+\infty} dz \sum_{j\in\mathcal{I}} |z, V_j[x(z)]\rangle \psi_j(z,t). \tag{23}$$

Using this result along with (21) and the definitions in (22) one finds that Schrödinger's equation is equivalent to a set of $\dim\mathcal{H}_0 = 2(2I+1)$ partial differential equations that can be written succinctly as follows:

$$\begin{aligned} &i\hbar\frac{\partial}{\partial t}\mathbf{\Psi}(z,t) \\ &\quad = \left\{-\frac{\hbar^2}{2M}\mathbb{K}(z) + \mathbb{V}(z) + \hbar\mathbb{D}(z,t) + \hbar\mathbb{G}(z,t) + \mathbb{L}(z)\right\} \\ &\qquad \times \mathbf{\Psi}(z,t) \quad (z,t\in\mathbb{R}). \end{aligned} \tag{24}$$

Here we have introduced the matrices

$$\begin{aligned} &\mathbb{K}_{jk}(z) = \delta_{jk}\frac{\partial^2}{\partial z^2}, \quad \mathbb{V}_{jk}(z) = \delta_{jk}\{Mg_0 z + V_j[x(z)]\}, \\ &\mathbb{D}_{jk}(z,t) = \delta_{jk}\delta_j[x(z),t], \quad \mathbb{G}_{jk}(z,t) = g_{jk}[x(z),t], \\ &\mathbb{L}_{jk}(z) = \mathcal{L}_{jk}(z), \quad \mathbf{\Psi}_j(z,t) = \psi_j(z,t), \end{aligned} \tag{25}$$

where $j,k = 1,2,\ldots,\dim\mathcal{H}_0 = 2(2I+1)$. Notice that $[-\hbar^2/(2M)]\mathbb{K}(z)$ represents the kinetic energy of the atom, $\mathbb{V}(z)$ is the sum of its internal energy plus its gravitational potential energy, $\hbar\mathbb{D}(z,t)$ represents a position- and time-dependent potential energy arising from the interaction with $\mathbf{B}_p(t)$, and $\hbar\mathbb{G}(z,t)$ and $\mathbb{L}(z)$ are couplings due to the interaction with $\mathbf{B}_p(t)$ and due to the dependence on position of the basis $\Gamma[x(z)]$, respectively.

It is important to notice that $\mathbb{L}(z)$ is a Hermitian matrix in the following sense:

$$[\mathbb{L}_{jk}(z)]^\dagger = \mathbb{L}_{kj}(z) \quad [j,k = 1,2,\ldots,2(2I+1)], \tag{26}$$

where the adjoint operator $[\mathbb{L}_{jk}(z)]^\dagger$ is calculated using the usual inner product of square integrable functions and taking boundary terms coming from integrating by parts to be zero (see Appendix D).

From (24) one finds that the original problem of an alkali-metal atom in the ground-state configuration with its center-of-mass motion quantized along the z axis, subject to a constant gravitational field, and interacting with a classical magnetic field of the form $B_{\mathrm{ST}}(z)\mathbf{z} + \mathbf{B}_p(t)$ is similar to a system of $\dim\mathcal{H}_0 = 2(2I+1)$ spinless particles moving in one dimension under the potentials $\mathbb{V}_{jj}(z) + \hbar\mathbb{D}_{jj}(z,t)$ and coupled through the interactions $\hbar\mathbb{G}_{jk}(z,t)$ and $\mathbb{L}_{jk}(z)$.

We now simplify (24). For the rest of the article we assume the following.

(1) $B_{\mathrm{ST}}(z) = \eta z$ ($z\in\mathbb{R}$) with $\eta > 0$ a constant with units G/cm. Appendix B gives an example of how ηz can be obtained from $B_{\mathrm{ST}}(z)$.

(2) The polarization $\mathbf{b}_p$ of $\mathbf{B}_p(t)$ is chosen depending on which levels $|V_{F,M_F}[x(z)]\rangle$ and $|V_{F',M_{F'}}[x(z)]\rangle$ one wishes to couple. We take

$$\mathbf{b}_p = \begin{cases} \mathbf{y} & \text{if} \quad |M_F - M_{F'}| = 1, \\ \mathbf{z} & \text{if} \quad |M_F - M_{F'}| = 0. \end{cases} \tag{27}$$

Here $\mathbf{y}$ is the unit vector in the positive y-axis direction.

(3) Let $j_0, j_1 \in \mathcal{I}$ with $j_0 \neq j_1$ and $\mathcal{V}$ be the region of space where the atom can be found with non-negligible probability during the time interval $[t_0,t_1]$ in which $\mathbf{B}_p(t)$ is applied. Then

$$g_{jk}[x(z),t] = 0, \tag{28}$$

for all $z\in\mathcal{V}$ and $t\in[t_0,t_1]$ if $(j,k)\notin\mathcal{I}_0 \equiv \{(j_0,j_1),(j_1,j_0)\}$. Here we are assuming that during the time interval $[t_0,t_1]$ the magnetic field $\mathbf{B}_p(t)$ couples the sets of states $\{|z,V_{j_0}[x(z)]\rangle : z\in\mathcal{V}\}$ and $\{|z,V_{j_1}[x(z)]\rangle : z\in\mathcal{V}\}$ resonantly, while all other transitions have $z\notin\mathcal{V}$ or are highly detuned and, therefore, their probability of occurrence is very small. Moreover, we consider only pulses; that is, we assume that $|t_1 - t_0|$ is sufficiently small because condition (28) is valid only for short times. The reason for this is that transitions that are initially far off resonance can become resonant and the transition that is initially resonant can become highly detuned due to the Zeeman effect as the atom moves.

We now use these assumptions to express (24) in terms of nondimensional quantities. First, take the characteristic length and time of the system to be $1/\kappa$ and $1/\Delta W$, respectively, where κ is defined to be

$$\kappa = \left(g_s\frac{\mu_B}{\hbar} + g_I\frac{\mu_N}{\hbar}\right)\frac{\eta}{\Delta W} > 0. \tag{29}$$

Notice that κ has units of 1/cm, ΔW has units of 1/s, and $x(z) = \kappa z$.

Now define the nondimensional quantities

$$\begin{aligned} \phi_j(x,\tau) &= \frac{1}{\sqrt{\kappa}}\psi_j(z,t)\Big|_{z=x/\kappa,t=\tau/\Delta W}, \\ V_j^0(x) &= \frac{1}{\hbar\Delta W}V_j[x(z)]\Big|_{z=x/\kappa}, \\ \delta_j^0(x,\tau) &= \frac{1}{\Delta W}\delta_j[x(z),t]\Big|_{z=x/\kappa,t=\tau/\Delta W}, \\ g_{jk}^0(x,\tau) &= \frac{1}{\Delta W}g_{jk}[x(z),t]\Big|_{z=x/\kappa,t=\tau/\Delta W}, \\ \epsilon &= \frac{\hbar^2}{2M}\frac{\kappa^2}{\hbar\Delta W} > 0, \end{aligned}$$

and

$$\begin{aligned} \omega_A^0 &= \frac{\omega_A}{\Delta W}, \quad \tau_0 = \Delta W t_0, \quad \tau_1 = \Delta W t_1, \\ \Omega_0(x) &= -\frac{B_0}{2\hbar\Delta W}\langle V_{j_0}(x)|\boldsymbol{\mu}\cdot\mathbf{b}_p|V_{j_1}(x)\rangle, \\ \Omega_0(x,\tau) &= \begin{cases} \Omega_0(x) & \text{if} \quad \tau_0 < \tau < \tau_1, \\ 0 & \text{if} \quad \tau \leqslant \tau_0 \text{ or } \tau \geqslant \tau_1. \end{cases} \\ \Omega_j'(x) &= -\frac{B_0}{2\hbar\Delta W}\langle V_j(x)|\boldsymbol{\mu}\cdot\mathbf{b}_p|V_j(x)\rangle, \\ \Omega_j'(x,\tau) &= \begin{cases} \Omega_j'(x) & \text{if} \quad \tau_0 < \tau < \tau_1, \\ 0 & \text{if} \quad \tau \leqslant \tau_0 \text{ or } \tau \geqslant \tau_1. \end{cases} \end{aligned}$$

and

$$\mathcal{L}^0_{jk}(x) = \sum_{F=F_\pm}\sum_{M_F=-F}^{F} \langle V_j(x)|k_0,F,M_F\rangle \times \left\{\left[\frac{\partial^2}{\partial x^2}\langle k_0,F,M_F|V_k(x)\rangle\right] + 2\left[\frac{\partial}{\partial x}\langle k_0,F,M_F|V_k(x)\rangle\right]\frac{\partial}{\partial x}\right\}. \quad (30)$$

Note that x is the nondimensional position, while $\tau = \Delta W t$ is the nondimensional time.

Using (30), one can express $|\psi(t)\rangle$ in (23) in the form

$$|\psi(t)\rangle = \int_{-\infty}^{+\infty} dx \sum_{j\in\mathcal{I}} \frac{1}{\sqrt{\kappa}}\left|\frac{x}{\kappa}, V_j(x)\right\rangle \phi_j(x,\Delta W t). \quad (31)$$

Finally, using (30) in (24) one finds that Schrödinger's equation is equivalent to

$$i\frac{\partial}{\partial\tau}\,\mathbf{\Phi}(x,\tau) = [-\epsilon\mathbb{K}^0(x) + \mathbb{V}^0(x) + \mathbb{D}^0(x,\tau) + \mathbb{G}^0(x,\tau) - \epsilon\mathbb{L}^0(x)] \times \mathbf{\Phi}(x,\tau) \qquad (x,\tau\in\mathbb{R}), \quad (32)$$

where we have introduced the matrices

$$\begin{aligned} \mathbf{\Phi}_j(x,\tau) &= \phi_j(x,\tau), \quad \mathbb{K}^0_{jk}(x) = \delta_{jk}\frac{\partial^2}{\partial x^2},\\ \mathbb{V}^0_{jk}(x) &= \delta_{jk}\left[V^0_j(x) + \frac{Mg_0}{\hbar\Delta W}\frac{x}{\kappa}\right],\\ \mathbb{D}^0_{jk}(x,\tau) &= \delta_{jk}\delta^0_j(x,\tau), \quad \mathbb{G}^0_{jk}(x,\tau) = g^0_{jk}(x,\tau),\\ \mathbb{L}^0_{jk}(x) &= \mathcal{L}^0_{jk}(x), \end{aligned} \quad (33)$$

for $j,k = 1,2,\ldots,\dim\mathcal{H}_0 = 2(2I+1)$. Note that (32) is just the nondimensional version of (24) using the special form $B_{\rm ST}(z) = \eta z$ and the characteristic length $1/\kappa$ and time $1/\Delta W$. Recall that (24) is valid for a general form of $B_{\rm ST}(z)$ [for example, it is valid for the nonlinear function given in (B2) in Appendix B and that constitutes an accurate approximation of an exact magnetic field with less stringent conditions (B3) than the special form $B_{\rm ST}(z) = \eta z$].

Using (28) and the definitions in (30), one can express $\mathbb{G}^0(x,\tau)$ as follows:

$$\mathbb{G}^0_{jk}(x,\tau) = \left[e^{i\omega^0_A(\tau-\tau_0)} + e^{-i\omega^0_A(\tau-\tau_0)}\right] \times \begin{cases} \Omega_0(x,\tau) & \text{if} \quad (j,k) = (j_0,j_1),\\ \Omega_0(x,\tau)^* & \text{if} \quad (j,k) = (j_1,j_0),\\ 0 & \text{if} \quad (j,k)\notin\mathcal{I}_0, \end{cases} \quad (34)$$

for $x,\tau\in\mathbb{R}$ and $j,k\in\mathcal{I}$. In this form it is seen explicitly that $\Omega_0(x,\tau)$ is the (nondimensional) position-dependent atom-$\mathbf{B}_p(t)$ coupling. Notice that the dependence on x arises from the fact that $|V_j(x)\rangle$ depends on x.

Similarly, it also follows that

$$\mathbb{D}^0_{jj}(x,\tau) = \Omega'_j(x,\tau)\left[e^{i\omega^0_A(\tau-\tau_0)} + e^{-i\omega^0_A(\tau-\tau_0)}\right]. \quad (35)$$

It is very important to realize that $\epsilon \ll 1$; that is, ϵ is a perturbation parameter in (32). This is shown explicitly in the next section to be a consequence of the long-wavelength approximation. Meanwhile, we illustrate this fact with a concrete example. For future reference, we note that ^{87}Rb has the parameters [17,19]

$$\begin{aligned} g_s &\simeq 2.002, \quad d_e \simeq 5.6a_0 \simeq 3\times10^{-10}\text{m},\\ g_I\frac{m_e}{m_p} &\simeq 0.001, \quad \Delta W \simeq 2\pi\times 6.835\times10^9\,\frac{1}{\text{s}},\\ I &= \frac{3}{2}, \quad M \simeq 1.45\times10^{-25}\text{kg}, \end{aligned} \quad (36)$$

where d_e is the average distance of the valence electron to the nucleus and a_0 is the Bohr radius. It follows that ^{87}Rb has

$$\epsilon = 1.42\times10^{-23}\eta^2, \quad (37)$$

where η is given in G/cm. Hence, ϵ is a perturbation parameter in (32) as long as one considers values of η smaller than 10^{11},10^{12} G/cm. Note that values $\eta\sim10^{11}$,10^{12} G/cm imply magnetic fields of the order of 10^{12} G, but these are only found in neutron stars [20]. Hence, ϵ is always a perturbation parameter as long as exotic environments such as neutron stars are excluded. In reality the model is no longer applicable for such high values of η, since the long-wavelength approximation breaks down. We emphasize that the magnitude of the magnetic field $B_{\rm ST}(z)$ is not an issue, it is the derivative η of $B_{\rm ST}(z)$ that determines if ϵ is a perturbation parameter or not.

Also, it is important to note that the presence of the perturbation parameter ϵ as a factor of the term $\mathbb{K}^0(x)$ associated with the kinetic energy in (33) does not imply that the kinetic energy is negligible. In fact, the expected value of the kinetic energy of the atom is calculated in Sec. IV and its expression shows that it can be larger than the gravitational potential plus internal energies. The presence of the perturbation parameter implies that the motion of the atom will tend to be *semiclassical* as it is explicitly seen in Sec. IV. The reason for this is that $\hbar$ is *small* in the system under consideration; that is, the quantity $\mathsf{h}_0 \equiv 2M\Delta W/\kappa^2$ with units of $\hbar$ can be formed with the characteristic length $1/\kappa$, time $1/\Delta W$, and mass M of the system and $\hbar$ is much smaller than h_0: $\epsilon = \hbar/\mathsf{h}_0 \ll 1$ [21].

The following sections present simplified forms of some of the matrices in (32) and a discussion of the validity of the long-wavelength approximation.

A. Validity of the long-wavelength approximation

The Hamiltonian (11) was derived under the long-wavelength approximation, so it is important to realize that this imposes limits on both the frequency ω_A of $\mathbf{B}_p(t)$ and the derivative η of $B_{\rm ST}(z)$. We first discuss the case of $\mathbf{B}_p(t)$.

Since $\mathbf{B}_p(t)$ corresponds to a monochromatic plane wave propagating along the positive x axis with wavelength $\lambda_A = 2\pi c/\omega_A$, the long-wavelength approximation requires that

$$\lambda_A \gg d_e \sim a_0, \quad (38)$$

where we have estimated the average distance d_e of the valence electron to the nucleus of the alkali-metal atom by the

Bohr radius a_0. In general, transitions between ground-state hyperfine sublevels in alkali-metal atoms have $\omega_A \leqslant 10^{13}$ 1/s. Therefore, $\lambda_A > 10^{-4}$ m, which is much larger than a_0. Hence, the long-wavelength approximation is valid. In particular, using (36) with $\omega_A = \Delta W$ we have $\lambda_A = 4.4 \times 10^{-2}$ m and $d_e \simeq 3 \times 10^{-10}$ m for ^{87}Rb. Clearly, the long-wavelength approximation is valid.

We now consider the case of $B_{\mathrm{ST}}(z) = \eta z$. If z is the (average) position of the nucleus and $z \pm d_e$ is the (average) position of the valence electron, then it must occur that

$$\left| \frac{B_{\mathrm{ST}}(z \pm d_e) - B_{\mathrm{ST}}(z)}{B_{\mathrm{ST}}(z)} \right| = \left| \frac{d_e}{z} \right| \ll 1, \tag{39}$$

for all z for the long-wavelength approximation to be valid. In other words, the magnetic field at the (average) position of the electron must be approximately equal to the magnetic field at the (average) position of the nucleus. Since this criterion depends on z it is better to demand that the internal energy at the (average) position of the nucleus must be approximately equal to the internal energy at the (average) position of the valence electron; that is, it must occur that

$$\left| \frac{V_{F,M_F}[\kappa(z \pm d_e)] - V_{F,M_F}(\kappa z)}{V_{F,M_F}(\kappa z)} \right| \ll 1, \tag{40}$$

for each z, $-F \leqslant M_F \leqslant F$, and $F = F_{\pm}$. To estimate (40) we take $z > 0$ and $F = M_F = F_+$. Using the definition of $V_{F_+,F_+}(\kappa z)$ in (8) one finds that the left side of (40) is less than or equal to $2\gamma_1 \kappa d_e$. Hence, using the definition of κ in (29) it follows that

$$\eta \ll \eta_{\mathrm{bound}} \equiv \frac{\Delta W}{d_e\left(g_s \frac{\mu_B}{\hbar} - 2I g_I \frac{\mu_N}{\hbar}\right)} \tag{41}$$

is a sufficient condition for (40) to be valid; that is, it is a sufficient condition for the long-wavelength approximation to be valid. In the case of ^{87}Rb one has

$$\eta_{\mathrm{bound}} = 8.2 \times 10^{10} \frac{\mathrm{G}}{\mathrm{cm}}. \tag{42}$$

Moreover, using (41) and (42) it follows from (37) that

$$\epsilon \ll 9.6 \times 10^{-2}. \tag{43}$$

Therefore, ϵ is always a perturbation parameter in (32) in the case of ^{87}Rb. We now treat the rest of the alkali-metal atoms.

Define

$$\begin{aligned} &\eta_{\max} = 10^{-n}\eta_{\mathrm{bound}}, \quad \kappa_{\max} = \frac{g_s\mu_B + g_I\mu_N}{\hbar \Delta W}\eta_{\max}, \\ &\epsilon_{\max} = \frac{\hbar^2}{2M}\left(\frac{\kappa_{\max}^2}{\hbar \Delta W}\right), \end{aligned} \tag{44}$$

with $n \geqslant 0$. Notice that $\kappa_{\max}$ and $\epsilon_{\max}$ are the maximum values κ and ϵ can have, since they are simply κ and ϵ with η replaced by $\eta_{\max}$.

Since $g_s \simeq 2$, one has

$$\frac{2I g_I \mu_N}{g_s \mu_B} \simeq I g_I \frac{m_e}{m_p}, \quad \frac{g_I \mu_N}{g_s \mu_B} \simeq g_I \frac{m_e}{2m_p}. \tag{45}$$

Hence, one can neglect $2I g_I \mu_N$ and $g_I \mu_N$ with respect to $g_s \mu_B$, and it follows from (44) that

$$\begin{aligned} &\eta_{\max} \simeq 10^{-n} \frac{\hbar \Delta W}{d_e g_s \mu_B}, \quad \kappa_{\max} \simeq \frac{10^{-n}}{d_e}, \\ &\epsilon_{\max} \simeq \frac{\hbar}{2M}\left(\frac{10^{-2n}}{d_e^2 \Delta W}\right). \end{aligned} \tag{46}$$

Since all alkali-metal atoms have $M > 10^{-27}$ kg and $d_e \geqslant a_0$, if we take $n = 3$ and $\Delta W \gtrsim 10^{10}$ 1/s it follows from (46) that

$$\epsilon_{\max} \lesssim 2 \times 10^{-3}. \tag{47}$$

Hence, $\epsilon \ll 1$ if $|2I g_I \mu_N| \ll g_s \mu_B$ and $\Delta W \gtrsim 10^{10}$ 1/s and the sufficient condition (41) for the long-wavelength approximation to be valid is used. We conclude that $\epsilon \ll 1$ if the long-wavelength approximation is valid.

B. Simplified form of $\mathcal{L}^0_{jk}(x)$

Recall that $\mathcal{L}^0_{jk}(x)$ arises from the use of the position-dependent basis $\Gamma[x(z)]$ in (17). Hence, using (8) it follows from (30) that

$$\begin{aligned} &\mathcal{L}^0_{jk}(x)\big|_{j=F_+,\pm F_+} = 0, \\ &\mathcal{L}^0_{jk}(x)\big|_{j=F_+,M_F} = \begin{cases} \alpha_0(M_F,x) & \text{if} \quad k = F_+, M_F, \\ -\alpha_1(M_F,x) & \text{if} \quad k = F_-, M_F, \\ 0 & \text{in another case}, \end{cases} \\ &\mathcal{L}^0_{jk}(x)\big|_{j=F_-,M_F} = \begin{cases} \alpha_1(M_F,x) & \text{if} \quad k = F_+, M_F, \\ \alpha_0(M_F,x) & \text{if} \quad k = F_-, M_F, \\ 0 & \text{in another case}, \end{cases} \end{aligned} \tag{48}$$

with

$$\begin{aligned} &\alpha_0(M_F,x) = -\frac{1}{4}\theta_x(M_F,x)^2, \\ &\alpha_1(M_F,x) = \frac{1}{2}\theta_{xx}(M_F,x) + \theta_x(M_F,x)\frac{\partial}{\partial x}, \\ &\theta_x(M_F,x) = -\frac{\sqrt{1-(M_F/F_+)^2}}{1 + 2(M_F/F_+)x + x^2}, \\ &\theta_{xx}(M_F,x) = 2\left(\frac{M_F}{F_+} + x\right)\frac{\sqrt{1-(M_F/F_+)^2}}{[1 + 2(M_F/F_+)x + x^2]^2}, \end{aligned} \tag{49}$$

for $k = 1,2,\ldots,\dim\mathcal{H}_0 = 2(2I+1)$ and $-F_- \leqslant M_F \leqslant F_-$. Here $\theta_x(M_F,x)$ and $\theta_{xx}(M_F,x)$ are the first and second partial derivatives with respect to x of the function $\theta(M_F,x)$ in (8).

From (48) it follows that $\mathbb{L}^0(x)$ has the block-diagonal form

$$\mathbb{L}^0(x) = \begin{pmatrix} \mathbb{O} & \mathbb{O} & \mathbb{O} & \ldots & \mathbb{O} \\ \mathbb{O} & \mathbb{M}_0(x) & \mathbb{O} & \ldots & \mathbb{O} \\ \mathbb{O} & \mathbb{O} & \mathbb{M}_1(x) & \ldots & \mathbb{O} \\ \vdots & \vdots & \vdots & & \vdots \\ \mathbb{O} & \mathbb{O} & \mathbb{O} & \ldots & \mathbb{M}_{2F_-}(x) \end{pmatrix}, \tag{50}$$

where $\mathbb{O}$ is the 2×2 zero matrix and

$$\mathbb{M}_j(x)=\begin{pmatrix}\alpha_0(F_- - j,x) & -\alpha_1(F_- - j,x)\\ \alpha_1(F_- - j,x) & \alpha_0(F_- - j,x)\end{pmatrix}, \tag{51}$$

for $j=0,1,\ldots,2F_-$. Recall that the ordering for $\Gamma[x(z)]$ is given in (19).

Observe that $\mathbb{L}^0(x)$ only couples $\phi_{F_+,M_F}(x,\tau)$ and $\phi_{F_-,M_F}(x,\tau)$ for $M_F=-F_-,\ldots,F_-$. The origin of this can be found in that $|k_0,F_\pm,M_F\rangle$ and $|V_{F_\pm,M_F}(x)\rangle$ are linear combinations of the same kets for each $-F_-\leqslant M_F\leqslant F_-$ [see (8) and (30)].

We emphasize that $\mathbb{L}^0(x)$ arises from the use of a position-dependent basis that comes from the interaction between the alkali-metal atom and the static magnetic field $B_{\rm ST}(z)\mathbf{z}$. Hence, its structure is independent $\mathbf{B}_p(t)$.

Finally, as a consequence of the Hermiticity condition (26) for $\mathbb{L}(z)$ one has a corresponding Hermiticity condition for $\mathbb{L}^0(x)$: $[\mathbb{L}^0_{jk}(x)]^\dagger=\mathbb{L}^0_{kj}(x)$ for each $j,k=1,2,\ldots,\dim\mathcal{H}_0=2(2I+1)$.

C. Simplified forms of $\mathbb{D}^0(x,\tau)$, $\Omega_0(x)$, and $\theta(M_F,x)$

One can further simplify $\mathbb{D}^0(x,\tau)$ if one evaluates the matrix element $\langle V_j(x)|\boldsymbol{\mu}\cdot\mathbf{b}_p|V_j(x)\rangle$. Using (7) and (8) it follows that this matrix element is zero if $\mathbf{b}_p=\mathbf{y}$. Therefore,

$$\mathbb{D}^0(x,\tau)=0 \quad \text{if} \quad \mathbf{b}_p=\mathbf{y}. \tag{52}$$

On the other hand, one finds that

$$\Omega'_j(x)=\frac{B_0}{2\hbar\Delta W}\times\begin{cases}\pm\left(\frac{g_s}{2}\mu_B-g_I I\mu_N\right),\\ -g_I\mu_N M_F\pm\frac{1}{2}\left(g_s\mu_B+g_I\mu_N\right)\cos\theta(M_F,x),\end{cases} \tag{53}$$

for all $x\in\mathbb{R}$ and $M_F=-F_-,\ldots,F_-$ if $\mathbf{b}_p=\mathbf{z}$. Here the first line corresponds to $j=F_+,\pm F_+$, while the second line corresponds to $j=F_\pm,M_F$.

It is important to note that $\Omega'_j(x)$ is a small quantity unless B_0 is on the order of 1 T. For example, for ^{87}Rb one has

$$|\Omega'_j(x)|\leqslant 1.03\times 10^{-4}B_0 \qquad (j\in\mathcal{I},x\in\mathbb{R}), \tag{54}$$

with B_0 given in gauss.

Using the definitions of $\theta(M_F,x)$ and $\Omega_0(x)$ given in (8) and (30), it can be shown that for $\tau_0<\tau<\tau_1$ one has

$$\begin{aligned}i\Omega_0(x,\tau)&=i\Omega_0(x),\\ &=\frac{B_0}{4\Delta W}\left(\frac{\mu_B}{\hbar}\right)\begin{cases}g_s\cos\left[\frac{\theta(F_-,x)}{2}\right]+g_I\frac{m_e}{m_p}\sqrt{2I}\sin\left[\frac{\theta(F_-,x)}{2}\right],\\ g_s\sin\left[\frac{\theta(-F_-,x)}{2}\right]+g_I\frac{m_e}{m_p}\sqrt{2I}\cos\left[\frac{\theta(-F_-,x)}{2}\right],\end{cases}\end{aligned} \tag{55}$$

with $j_0=F_+,F_+$ and $j_1=F_-,F_-$ for the first line and $j_0=F_+,-F_+$ and $j_1=F_-,-F_-$ for the second line.

Also, using the definition of $\theta(M_F,x)$ given in (8) it follows that

$$\begin{aligned}\cos\left[\frac{\theta(M_F,x)}{2}\right]&=\frac{1}{\sqrt{2}}\sqrt{1+\frac{\frac{M_F}{F_+}+x}{\sqrt{1+2\frac{M_F}{F_+}x+x^2}}},\\ \sin\left[\frac{\theta(M_F,x)}{2}\right]&=\frac{1}{\sqrt{2}}\sqrt{1-\frac{\frac{M_F}{F_+}+x}{\sqrt{1+2\frac{M_F}{F_+}x+x^2}}},\end{aligned} \tag{56}$$

for $-F_-\leqslant M_F\leqslant F_-$.

D. A criterion to select a transition

In (28) we kept the discussion at a general level and we did not specify which transition was chosen; that is, we did not choose particular values for j_0 and j_1. While some transitions may exhibit certain properties that may make them more advantageous than others such as a simpler experimental preparation of the initial state or a $V_j[x(z)]$ that can be approximated by a harmonic oscillator potential for small $x(z)$, we concentrate just on presenting a criterion that can be used to establish which transition gives rise to the best phase-space selector (that is, the best selections in position and velocity). We need states with the biggest change in resonant frequency for a given displacement, that is, that have the largest value of

$$\left|\frac{dV^0_{j_0}}{dx}(x)-\frac{dV^0_{j_1}}{dx}(x)\right|. \tag{57}$$

Here we divided by $\hbar\Delta W$ in order to have nondimensional quantities.

We expect that the allowed transitions that have the largest value of (57) have

$$(j_0;j_1)=\begin{cases}(F_+,F_+\,;F_-,F_-) & \text{for} \quad x>0,\\ (F_+,-F_+;F_-,-F_-) & \text{for} \quad x<0,\end{cases} \tag{58}$$

since they involve the stretched states and these are the most sensitive to the magnetic field. We verified this claim for ^{87}Rb. Moreover, experimentally, it is easier to prepare atoms in the states $|V_j[x(z)]\rangle$ with $j=j_0,j_1$ given in (58).

IV. EVOLUTION BEFORE THE PULSE

In this section we restrict to $0\leqslant t\leqslant t_0$ so that $\mathbf{B}_p(t)=0$ during this time interval. The Schrödinger equation is solved in the first section, while the evolution is analyzed in the second section. The reader interested only in the analysis can jump to the second section.

A. Solution of the Schrödinger equation

Since $\mathbf{B}_p(t)=0$ during the time interval $0\leqslant t\leqslant t_0$ [see (13)], it follows from (22), (30), and (33) that $\mathbb{D}^0(x,\tau)=$

$\mathbb{G}^0(x,\tau)=0$ for $x\in\mathbb{R}$ and $0\leqslant t\leqslant t_0$. Hence, (32) takes the form

$$i\frac{\partial}{\partial\tau}\,\mathbf{\Phi}(x,\tau)=[\mathbb{V}^0(x)-\epsilon\mathbb{K}^0(x)-\epsilon\mathbb{L}^0(x)]\,\mathbf{\Phi}(x,\tau). \quad (59)$$

Using the structure of the matrices on the right one finds that (59) is equivalent to the following set of equations:

$$i\frac{\partial}{\partial\tau}\phi_{F_+,\pm F_+}(x,\tau) =\left[-\epsilon\frac{\partial^2}{\partial x^2}+\frac{1}{2}+\left(\pm\gamma_1+\frac{Mg_0}{\hbar\Delta W\kappa}\right)x\right]\phi_{F_+,\pm F_+}(x,\tau) \quad (60)$$

for the stretched states and

$$i\frac{\partial}{\partial\tau}\begin{pmatrix}\phi_{F_+,M_F}(x,\tau)\\ \phi_{F_-,M_F}(x,\tau)\end{pmatrix}=\mathbb{A}(M_F,x)\begin{pmatrix}\phi_{F_+,M_F}(x,\tau)\\ \phi_{F_-,M_F}(x,\tau)\end{pmatrix}$$

for $-F_-\leqslant M_F\leqslant F_-$. Here

$$\mathbb{A}(M_F,x)=\begin{pmatrix}V^0_{F_+,M_F}(x)+\frac{Mg_0}{\hbar\Delta W\kappa}x & 0\\ 0 & V^0_{F_-,M_F}(x)+\frac{Mg_0}{\hbar\Delta W\kappa}x\end{pmatrix} -\epsilon\begin{pmatrix}\frac{\partial^2}{\partial x^2}+\alpha_0(M_F,x) & -\alpha_1(M_F,x)\\ \alpha_1(M_F,x) & \frac{\partial^2}{\partial x^2}+\alpha_0(M_F,x)\end{pmatrix}, \quad (61)$$

with the definitions in (8), (30), and (49). Notice that $\phi_j(x,\tau)$ evolves independently of the rest for $j=(F_+,\pm F_+)$, while $\phi_{F_+,M_F}(x,\tau)$ and $\phi_{F_-,M_F}(x,\tau)$ are weakly coupled ($-F_-\leqslant M_F\leqslant F_-$). This weak coupling arises from the position-dependent basis $\Gamma[x(z)]$ used to write the Schrödinger equation.

We now focus our attention on $\phi_j(x,\tau)$ for $j=F_+,\pm F_+$. As explained in Sec. IIID, these are the states with the highest sensitivity to the magnetic field and give rise to the best phase-space selector.

Equations (60) have the generic form

$$i\frac{\partial}{\partial\tau}\phi(x,\tau)=\left(-\epsilon\frac{\partial^2}{\partial x^2}+q_1+q_2x\right)\phi(x,\tau), \quad (62)$$

with $q_1,q_2\in\mathbb{R}$.

Notice that the equation for $\phi_{F_+,\pm F_+}(x,\tau)$ is recovered by taking $\phi_{F_+,\pm F_+}(x,\tau)=\phi(x,\tau)$ and

$$q_1=\frac{1}{2},\quad q_2=\left(\frac{Mg_0}{\hbar\Delta W\kappa}\pm\gamma_1\right). \quad (63)$$

We now solve (62) subject to the initial condition $\phi(x,0)$ and assuming that $\phi(\cdot,\tau)\in S(\mathbb{R})$ and that $(\partial/\partial\tau)\mathcal{F}_x[\phi(x,\tau)]=\mathcal{F}_x[(\partial/\partial\tau)\phi(x,\tau)]$ for each $\tau\in\mathbb{R}$. Here $\mathcal{F}_x$ denotes the Fourier transform with respect to x and $S(\mathbb{R})$ is the space of infinitely differentiable complex-valued functions defined on $\mathbb{R}$ that decrease rapidly at infinity [22].

Since $\phi(\cdot,\tau)\in S(\mathbb{R})$ and $(\partial/\partial\tau)\mathcal{F}_x[\phi(x,\tau)]=\mathcal{F}_x[(\partial/\partial\tau)\phi(x,\tau)]$ for each $\tau\in\mathbb{R}$, we can take the Fourier transform with respect to x on both sides of (62) to obtain the equivalent equation

$$\frac{\partial}{\partial\tau}\hat{\phi}(k,\tau)-q_2\frac{\partial}{\partial k}\hat{\phi}(k,\tau)=-i(q_1+\epsilon k^2)\hat{\phi}(k,\tau) \quad (64)$$

for $k,\tau\in\mathbb{R}$. Here $\hat{\phi}(k,\tau)$ is the Fourier transform of $\phi(x,\tau)$ with respect to x; that is,

$$\hat{\phi}(k,\tau)=\frac{1}{\sqrt{2\pi}}\int_{-\infty}^{+\infty}dx\phi(x,\tau)e^{-ikx}, \quad (65)$$

for $k,\tau\in\mathbb{R}$. By taking the Fourier transform we have changed a second-order linear partial differential equation into a first-order one.

Using the method of characteristics [23] one can solve Eq. (64). We omit the details and write only the solution

$$\hat{\phi}(k,\tau)=\hat{\phi}(k+q_2\tau,0) \times\exp\left[-iq_1\tau+i\frac{\epsilon}{3q_2}k^3-i\frac{\epsilon}{3q_2}(k+q_2\tau)^3\right]. \quad (66)$$

Taking the inverse Fourier transform of (66) and making a change of variables one arrives at the solution of (62):

$$\phi(x,\tau)=\exp\left[-iq_1\tau-iq_2\tau\left(x+\frac{\epsilon}{3}q_2\tau^2\right)\right] \times\frac{1}{\sqrt{2\pi}}\int_{-\infty}^{+\infty}dk\hat{\phi}(k,0) \times\exp[-i\epsilon\tau k^2+ik(\epsilon q_2\tau^2+x)]. \quad (67)$$

Note that $\phi(x,\tau)$ in (67) is indeed in $S(\mathbb{R})$ for each $\tau\in\mathbb{R}$ if $\phi(x,0)\in S(\mathbb{R})$.

In the following we assume that $\psi(z,0)$ is a coherent state wave packet [16]; that is,

$$\psi(z,0)=\left[\frac{1}{2\pi\Delta Z(0)^2}\right]^{1/4}\exp\left\{-\frac{1}{4}\left[\frac{z-z_0}{\Delta Z(0)}\right]^2+i\frac{p_0}{\hbar}z\right\}. \quad (68)$$

Using (30) it follows from (68) that

$$\phi(x,0)=\frac{1}{\sqrt{\kappa}}\psi\left(\frac{x}{\kappa},0\right). \quad (69)$$

Now substitute (68) and (69) in (67) and evaluate the integral by the method of residues. The result is

$$\phi(x,\tau)=\left[\frac{1}{2\pi\sigma_x(\tau)^2}\right]^{1/4}\exp\left\{-\frac{1}{4}\frac{[x-\zeta(\tau)]^2}{\sigma_x(\tau)^2} +i\Theta_{\rm p}(x,\tau)-\frac{i}{2}\tan^{-1}\left[\frac{\epsilon\tau}{\sigma_x(0)^2}\right]\right\}. \quad (70)$$

Here we introduced the nondimensional quantities

$$\sigma_x(0)=\kappa\Delta Z(0),\quad \rho_0=\frac{p_0}{\hbar\kappa},\quad x_0=\kappa z_0,$$

$$\sigma_x(\tau)=\sqrt{\sigma_x(0)^2+\left[\frac{\epsilon\tau}{\sigma_x(0)}\right]^2},$$

$$\zeta(\tau)=x_0+2\rho_0(\epsilon\tau)-q_2(\epsilon\tau^2),$$

and

$$\Theta_{\rm p}(x,\tau) = -\tau\left(q_1 + \frac{\epsilon}{3}q_2^2\tau^2\right) + \frac{\sigma_x(0)^2}{\sigma_x(\tau)^2}(\rho_0 - q_2\tau)(x - \rho_0\epsilon\tau) + \frac{\epsilon\tau}{4\sigma_x(\tau)^2\sigma_x(0)^2}\Big[(x-x_0)^2 + 4\rho_0 x_0\epsilon\tau - 2q_2\epsilon\tau^2\left(x + x_0 - \frac{q_2}{2}\epsilon\tau^2\right)\Big]. \quad (71)$$

Notice that $\phi(x,\tau)$ is a Gaussian wave packet whose standard deviation $\sigma_x(\tau)$ increases just like a free particle Gaussian wave packet (the free particle case is obtained by taking $q_1 = q_2 = 0$).

In the following section the result in (70) is used to determine the state of the system $|\psi(t)\rangle$ for $0 \leqslant t \leqslant t_0$.

B. Evolution of the atom

Suppose that the state of the system at time $t = 0$ is

$$|\psi(0)\rangle = \int_{-\infty}^{+\infty} dx \frac{1}{\sqrt{\kappa}}\left|\frac{x}{\kappa}, V_{j_0}(x)\right\rangle \phi(x,0), \quad (72)$$

with $j_0 = F_+, F_+$ or $F_+, -F_+$ and $\phi(x,0)$ the coherent state wave packet in (68) and (69). Notice that we used (31) to write (72).

It follows from (72) and the results of the previous section that the state of the system at time $0 \leqslant t \leqslant t_0$ is given by

$$|\psi(t)\rangle = \int_{-\infty}^{+\infty} dx \frac{1}{\sqrt{\kappa}}\left|\frac{x}{\kappa}, V_{j_0}(x)\right\rangle \phi(x,\Delta W t), \quad (73)$$

where $\phi(x,\tau)$ is the Gaussian wave packet given in (70) and (71).

Using (73) and the definition of $|z, V_{j_0}[x(z)]\rangle$ in (8) and (20) it is straightforward to show that the expected values of position $\langle Z\rangle(t)$ and momentum $\langle P_z\rangle(t)$ and the dispersions (or standard deviations) of position $\Delta Z(t)$ and momentum $\Delta P_z(t)$ are given by

$$\begin{aligned}
\langle Z\rangle(t) &= \frac{\zeta(\Delta W t)}{\kappa} = z_0 + \frac{p_0}{M}t - \frac{1}{2}g_{\rm eff}t^2,\\
\Delta Z(t) &= \frac{1}{\kappa}\sigma_x(\Delta W t),\\
&= \sqrt{\Delta Z(0)^2 + \left[\frac{\hbar}{2M\Delta Z(0)}\right]^2 t^2}, \quad (74)\\
\langle P_z\rangle(t) &= M\frac{d}{dt}\langle Z\rangle(t),\\
\Delta P_z(t) &= \Delta P_z = \frac{\hbar}{2\Delta Z(0)},
\end{aligned}$$

where $z_0 = \langle Z\rangle(0)$, $p_0 = \langle P_z\rangle(0)$, $\zeta(\Delta W t)$ is the nondimensional expected value of position, and $\sigma_x(\Delta W t)$ is the nondimensional standard deviation of position. Also,

$$g_{\rm eff} = g_0 \pm g', \quad g' = \frac{\hbar}{2M}\left(g_s\frac{\mu_B}{\hbar} - 2I g_I\frac{\mu_N}{\hbar}\right)\eta. \quad (75)$$

The $\pm$ sign in (75) is chosen according to $j_0 = F_+, \pm F_+$.

Moreover, the probability density functions (pdf's) of position and momentum are found to be respectively given by

$$\begin{aligned}
f_{\rm Z}(z,t) &= \kappa|\phi(\kappa z, \Delta W t)|^2\\
&= \frac{1}{\sqrt{2\pi\Delta Z(t)^2}}\exp\left[-\frac{1}{2}\left(\frac{z - \langle Z\rangle(t)}{\Delta Z(t)}\right)^2\right], \quad (76)\\
f_{\rm P}(p,t) &= \frac{1}{\sqrt{2\pi\Delta P_z^2}}\exp\left[-\frac{1}{2}\left(\frac{p - \langle P_z\rangle(t)}{\Delta P_z}\right)^2\right],
\end{aligned}$$

for $z, p \in \mathbb{R}$ and $t \in [0, t_0]$.

From (59) and (60) one knows that the Schrödinger equation of the system for the initial state in (72) and for $t \in [0, t_0]$ reduces to that of a single spinless particle moving in one dimension under an effective potential that includes the gravitational potential energy of the atom and its internal energy [we include the interaction energy with the static magnetic field $B_{\rm ST}(z)\mathbf{z} = \eta z\mathbf{z}$ in the internal energy]. From the aforementioned equations it follows that this effective potential is given by

$$Mg_0 z + V_{j_0}(\kappa z) = \frac{\hbar\Delta W}{2} + Mg_{\rm eff}z, \quad (77)$$

with $j_0 = F_+, \pm F_+$. Hence, from (74) we conclude that $\langle Z\rangle(t)$ and $\langle P_z\rangle(t)$ follow the classical equations of motion; that is, they are equal to the position and momentum of a classical point particle of mass M and position $z(t)$ that is subject to the potential in (77) and that satisfies the initial conditions $z(0) = z_0$ and $(dz/dt)(0) = p_0/M$. Notice that the internal energy of the atom [including the interaction energy with $B_{\rm ST}(z)\mathbf{z}$] gives rise to an augmented acceleration of gravity $g_{\rm eff} = g_0 + g' > g_0$ in the case $j_0 = F_+, F_+$. On the other hand, it gives rise to a decreased acceleration of gravity $g_{\rm eff} = g_0 - g' < g_0$ for $j_0 = F_+, -F_+$. In the latter case, $g_{\rm eff}$ can become negative for sufficiently large values of η and, hence, the atom can be accelerated upwards even in the presence of gravity. For ^{87}Rb one has

$$g_{\rm eff} = 9.8 \pm 0.64\eta, \quad (78)$$

where η is given in G/cm and $g_{\rm eff}$ is in units of m/s^2. If $\eta = 100$ G/cm, then one has the augmented (reduced) value $g_{\rm eff} = 73.8$ m/s^2 ($g_{\rm eff} = -54.2$ m/s^2).

Notice that both the position and momentum pdf's are Gaussians with means equal to $\langle Z\rangle(t)$ and $\langle P_z\rangle(t)$, respectively. Also, the dispersion ΔP_z in momentum is constant in time. This is due to the fact that the *force* associated with the effective potential (77) is independent of z. The dispersion $\Delta Z(t)$ in position is equal to that of a freely evolving Gaussian wave packet. Hence, there is no compression of the position pdf as it is reflected downwards by the potential $V_{j_0}(\kappa z) + Mg_0 z$ in the case $j_0 = F_+, F_+$ (compare this with the evolution of Gaussian wave packets under the potential e^{-z^2} [24]). It is important to notice that $\Delta Z(t)$ does not depend on the value of η; that is, it is independent of the magnetic field $\eta z\mathbf{z}$. Nevertheless, the same is not true of the nondimensional dispersion $\sigma_x(\Delta W t) = \kappa\Delta Z(t)$. If η is replaced by $\lambda\eta$ ($\lambda > 0$), then $\sigma_x(\tau)$ is replaced by $\lambda\sigma_x(\tau)$.

We mention that using Ehrenfest's theorem and that the atom moves under the effective potential (77) (a polynomial of degree 1 in z), one could have also anticipated that $\langle Z\rangle(t)$ and $\langle P_z\rangle(t)$ follow the classical equations of motion.

To end this section we consider the expected values $\langle P_z^2/(2M)\rangle(t)$ of the kinetic energy, $\langle \mathsf{V}\rangle(t)$ of the effective potential energy, and $\langle H\rangle(t)$ of the total energy as well as the dispersion (or standard deviation) $\Delta H(t)$ of the total energy. Again, using (73) and the definition of $|z,V_{j_0}[x(z)]\rangle$ in (8) and (20) it is straightforward to show that

$$\begin{aligned}\left\langle \frac{P_z^2}{2M}\right\rangle(t) &= \frac{\langle P_z\rangle(t)^2}{2M} + \frac{\Delta P_z^2}{2M},\\ \langle \mathsf{V}\rangle(t) &= \frac{\hbar\Delta W}{2} + Mg_{\rm eff}\langle Z\rangle(t),\\ \langle H\rangle(t) &= \frac{\langle P_z\rangle(0)^2}{2M} + \frac{\Delta P_z^2}{2M} + \frac{\hbar\Delta W}{2} + Mg_{\rm eff}\langle Z\rangle(0),\\ \Delta H(t)^2 &= \left(\frac{\Delta P_z^2}{2M}\right)^2 + [Mg_{\rm eff}\Delta Z(0)]^2\\ &\quad + \frac{\Delta P_z^2}{2M}\left[\frac{\Delta P_z^2}{2M} + 4\frac{\langle P_z\rangle(0)^2}{2M}\right].\end{aligned} \tag{79}$$

Here $\mathsf{V} = Mg_0Z + H_A - \boldsymbol{\mu}\cdot B_{\rm ST}(Z)\mathbf{z}$ is the sum of the gravitational potential energy of the atom plus its internal energy plus its interaction with $B_{\rm ST}(z)\mathbf{z}$ energy. Also, observe from (11) that $H(t) = P_z^2/(2M) + \mathsf{V}$ for all $t\in[0,t_0]$.

Notice that the expected value of the kinetic energy is equal to the classical kinetic energy plus a term associated with the dispersion in momentum, while the expected value of the gravitational potential plus internal plus interaction with $B_{\rm ST}(z)\mathbf{z}$ energies is equal to the classical energy associated with the effective potential in (77). As a consequence, $\langle H\rangle(t)$ is equal to the classical energy (kinetic energy of the center-of-mass motion plus effective potential energy) plus the correction $\Delta P_z^2/(2M)$ due to the dispersion in momentum. Finally, the square of the standard deviation $\Delta H(t)^2$ of the energy is equal to the square of the *fluctuation* in the kinetic energy $[\Delta P_z^2/(2M)]^2$ plus the square of the *fluctuation* in the effective potential energy $[Mg_{\rm eff}\Delta Z(0)]^2$ plus a correction embodied by the third term on the right in the equation for $\Delta H(t)^2$ in (79).

V. EVOLUTION DURING THE PULSE

In this section we determine the evolution of the system during the application of the microwave pulse $\mathbf{B}_p(t)$; that is, we restrict to the time interval $t_0 < t < t_1$.

As before, we take j_0 and j_1 given in (58). According to (27) and (52) the polarization $\mathbf{b}_p$ of $\mathbf{B}_p(t)$ is $\mathbf{y}$ and $\mathbb{D}^0(x,\tau) = 0$.

We assume that the state of the system at time $t = 0$ is given in (72). Hence, the state of the system at time t_0 is given in (73) with $t = t_0$.

In the first section below an approximate solution of the Schrödinger equation is derived with the rotating wave approximation (RWA) and perturbation theory. Its accuracy and the validity of the RWA are discussed in the following two sections. The reader interested in the details and in the regime of validity of the approximate solution should go through them. Otherwise, the reader can take on faith the results below and jump to Sec V D.

The state of the system at time $t = \tau/\Delta W \in (t_0,t_1)$ is given by

$$\begin{aligned}|\psi(t)\rangle = \int_{-\infty}^{+\infty} dx\Bigg\{&\frac{1}{\sqrt{\kappa}}\left|\frac{x}{\kappa},V_{j_0}(x)\right\rangle\phi_{j_0}(x,\tau)\\ &+\frac{1}{\sqrt{\kappa}}\left|\frac{x}{\kappa},V_{j_1}(x)\right\rangle\phi_{j_1}(x,\tau)\Bigg\},\end{aligned} \tag{80}$$

where

$$\begin{aligned}\begin{pmatrix}\phi_{j_0}(x,\tau)\\ \phi_{j_1}(x,\tau)\end{pmatrix} &\simeq \begin{pmatrix}e^{-i\omega_0^0(\tau-\tau_0)}\phi_{00}^0(x,\tau)\\ e^{-i\omega_1^0(\tau-\tau_0)}\phi_{10}^0(x,\tau)\end{pmatrix},\\ \begin{pmatrix}\phi_{00}^0(x,\tau)\\ \phi_{10}^0(x,\tau)\end{pmatrix} &= \phi(x,\tau_0)e^{-i\Omega_p(x)(\tau-\tau_0)}\begin{pmatrix}\mathbb{U}_{11}(x,\tau)^*\\ -\mathbb{U}_{21}(x,\tau)\end{pmatrix},\end{aligned} \tag{81}$$

and

$$\begin{aligned}\mathbb{U}_{11}(x,\tau) &= \cos\left[\frac{\Omega_R(x)}{2}(\tau-\tau_0)\right]\\ &\quad + i\cos[\Theta_R(x)]\sin\left[\frac{\Omega_R(x)}{2}(\tau-\tau_0)\right],\\ \mathbb{U}_{21}(x,\tau) &= -\gamma_3(x)\sin[\Theta_R(x)]\sin\left[\frac{\Omega_R(x)}{2}(\tau-\tau_0)\right].\end{aligned} \tag{82}$$

Here we have introduced the following nondimensional quantities

$$\begin{aligned}\delta_{00}(x) &= V_{j_0}^0(x) - V_{j_1}^0(x) - \omega_A^0,\\ \Omega_p(x) &= \frac{1}{2}\left[V_{j_0}^0(x) - \omega_0^0 + V_{j_1}^0(x) - \omega_1^0\right] + \frac{Mg_0}{\hbar\Delta W\kappa}x,\\ \Omega_R(x) &= \sqrt{\delta_{00}(x)^2 + 4|\Omega_0(x)|^2},\\ \Theta_R(x) &= \cos^{-1}\left[\frac{\delta_{00}(x)}{\Omega_R(x)}\right]\in[0,\pi),\\ \gamma_3(x) &= \mathrm{sgn}[i\Omega_0(x)],\quad \zeta_R(\tau) = x_{0R} + 2\rho_{0R}\epsilon\tau - q_2\epsilon\tau^2,\\ \omega_l^0 &= V_{j_l}^0(x) + \frac{Mg_0}{\hbar\Delta W\kappa}x\Big|_{x=\zeta_R(\tau_0)},\quad \omega_A^0 = \omega_0^0 - \omega_1^0,\end{aligned} \tag{83}$$

where x_{0R} and ρ_{0R} are nondimensional real numbers, q_2 is the nondimensional quantity given in (63), and $l = 0,1$, and 2. Also, $j_2 = F_+,\pm F_-$ with the sign chosen according to $j_0 = F_+,\pm F_+$. The index j_2 is only used to deduce the approximate solution of the Schrödinger equation.

From (55) it is clear that $i\Omega_0(x)$ is a real quantity [recall that $\Omega_0(x)$ is the nondimensional atom-$\mathbf{B}_p(t)$ coupling that it is defined in (30) and simplified in (55) for the choice of j_0 and j_1 given in (58)]. Moreover, one can prove that

$$i\Omega_0(x) > 0, \tag{84}$$

if j_0, j_1, x satisfy (58) and either $g_I > 0$ or $g_s \geqslant |g_I|m_e\sqrt{2I}/m_p$. For ^{87}Rb the last condition is satisfied; see (36).

Also, $\delta_{00}(x)$ plays the role of a (nondimensional) position-dependent detuning, while $\Omega_R(x)$ is a (nondimensional) position-dependent Rabi frequency. The position-dependent Rabi angular frequency (units of rad/s) is given by $\Delta W\Omega_R(x)$. This is seen explicitly in Sec. VD below.

Observe that the nondimensional angular frequency ω_A^0 of $\mathbf{B}_p(t)$ [see (30)] is defined to be the nondimensional angular transition frequency between the levels $|z,V_{j_0}[x(z)]\rangle$ and $|z,V_{j_1}[x(z)]\rangle$ with $z=\zeta_R(\tau_0)/\kappa$. Comparing $\zeta_R(\tau)/\kappa$ with $\zeta(\tau)/\kappa$ in (74), it follows that $\zeta_R(\tau)/\kappa$ with $0\leqslant\tau\leqslant\tau_0$ is the expected value of the position of an atom whose expected values of position and momentum at time $t=0$ are x_{0R}/κ and $M(2\rho_{0R}\epsilon\Delta W)/\kappa=\hbar\kappa\rho_{0R}$, respectively. Therefore, the magnetic field $\mathbf{B}_p(t)$ will be resonant with the desired transition if $\zeta_R(\tau_0)=\zeta(\tau_0)$ and the atom is well localized around its expected value of position $\langle Z\rangle(t_0)=\zeta(\tau_0)/\kappa$ in (74). Notice that $\zeta_R(\tau_0)/\kappa$ plays the role of a *resonant position*.

We emphasize that we defined the angular frequency of $\mathbf{B}_p(t)$ to be resonant with the transition (58) if the atom is well localized around $\zeta(\tau_0)/\kappa=\zeta_R(\tau_0)/\kappa$. This is evidenced since the detuning is $\delta_{00}[\zeta_R(\tau_0)]=0$. In fact, from (83) one has

$$\begin{aligned}&\cos\Theta_R[\zeta_R(\tau_0)]=0,\quad \Omega_R[\zeta_R(\tau_0)]=2|\Omega_0[\zeta_R(\tau_0)]|,\\&\sin\Theta_R[\zeta_R(\tau_0)]=1,\quad \delta_{00}[\zeta_R(\tau_0)]=0.\end{aligned}\tag{85}$$

Also, notice that ω_l^0 is the (nondimensional) effective potential energy of an atom that is well localized around $\zeta_R(\tau_0)/\kappa$ and in the internal state $|V_{j_l}[\zeta_R(\tau_0)]\rangle$.

The approximate solution in (80) and (81) is called *the first-term approximation* and it will be used in the rest of the article. Observe that the first-term approximation corresponds to what one imagines a pulse to be like: a sudden application of a (magnetic) field that affects the atom and that is so brief that the atom barely moves. That the atom does not move during the pulse in the first-term approximation can be seen by calculating the position pdf $f_Z(z,t)$ of the atom from (80) and (81). It is given by

$$\begin{aligned}f_Z(z,t)&=\kappa|\phi_{j_0}(\kappa z,\tau)|^2+\kappa|\phi_{j_1}(\kappa z,\tau)|^2,\\&\simeq\kappa|\phi(\kappa z,\tau_0)|^2,\end{aligned}\tag{86}$$

for $z\in\mathbb{R}$ and $t=\tau/\Delta W\in[t_0,t_1]$.

A. Solution of the Schrödinger equation

In this section we solve the Schrödinger equation in the time interval $t_0<t<t_1$. Since the state of the system at time $t=t_0$ is given in (73) with $t=t_0$, it follows from (32) and (73) that one has to solve the equation

$$\begin{aligned}i\frac{\partial}{\partial\tau}\,\mathbf{\Phi}(x,\tau)=&[-\epsilon\mathbb{K}^0(x)+\mathbb{V}^0(x)+\mathbb{G}^0(x,\tau)-\epsilon\mathbb{L}^0(x)]\\&\times\ \mathbf{\Phi}(x,\tau),\end{aligned}\tag{87}$$

subject to the initial conditions

$$\mathbf{\Phi}_j(x,\tau_0)=\delta_{jj_0}\phi(x,\tau_0).\tag{88}$$

Recall that at the beginning of this section it was observed that $\mathbb{D}^0(x,\tau)=0$ due to the choice of polarization of $\mathbf{B}_p(t)$.

Notice from (33) that $\mathbb{K}^0(x)$ and $\mathbb{V}^0(x)$ are diagonal. Also, from (34) it follows that $\mathbb{G}^0(x,\tau)$ only couples $\phi_{j_0}(x,\tau)$ and $\phi_{j_1}(x,\tau)$. Furthermore, from (50) and the observation made in the paragraph below (51) one has that $\mathbb{L}^0(x)$ only couples $\phi_{j_1}(x,\tau)$ and $\phi_{j_2}(x,\tau)$ with

$$j_2=\ F_+,\pm F_-,\tag{89}$$

and the sign chosen according to $j_1=F_-,\pm F_-$. Hence, it follows from (87) and the initial conditions in (88) that

$$\phi_j(x,\tau)=0\quad(j\neq j_0,j_1,j_2).\tag{90}$$

These wave functions started out as zero and remain zero because they are not coupled to $\phi_{j_l}(x,\tau)$ for $l=0,1,2$.

Only the equations for $\phi_j(x,\tau)$ with $j=j_0,j_1,j_2$ have to be solved. We now make a transformation in order to be able to perform the RWA.

Define

$$\begin{aligned}\phi_{j_l}^0(x,\tau)&=e^{i\omega_l^0(\tau-\tau_0)}\phi_{j_l}(x,\tau),\\\mathbb{M}_{ll}(x)&=V_{j_l}^0(x)-\omega_l^0+\frac{Mg_0}{\hbar\Delta W\kappa}x,\\\mathbb{M}_{13}(x,\tau)&=\Omega_0(x)\big[1+e^{i2\omega_A^0(\tau-\tau_0)}\big],\\\mathbb{N}_{22}(x,M_F)&=-\frac{\partial^2}{\partial x^2}-\alpha_0(M_F,x),\\\mathbb{N}_{23}(x,M_F)&=\alpha_1(M_F,x)e^{i(\omega_2^0-\omega_1^0)(\tau-\tau_0)},\\\mathbb{N}_{32}(x,M_F)&=-\alpha_1(M_F,x)e^{-i(\omega_2^0-\omega_1^0)(\tau-\tau_0)},\end{aligned}\tag{91}$$

and

$$\begin{aligned}\mathbb{M}_0(x,\tau)&=\begin{pmatrix}\mathbb{M}_{00}(x)&0&\mathbb{M}_{13}(x,\tau)\\0&\mathbb{M}_{22}(x)&0\\\mathbb{M}_{13}(x,\tau)^*&0&\mathbb{M}_{11}(x)\end{pmatrix},\\\mathbb{M}_1(x,\tau)&=\begin{pmatrix}-\frac{\partial^2}{\partial x^2}&0&0\\0&\mathbb{N}_{22}(x,M_F)&\mathbb{N}_{23}(x,M_F)\\0&\mathbb{N}_{32}(x,M_F)&\mathbb{N}_{22}(x,M_F)\end{pmatrix},\end{aligned}\tag{92}$$

for each $l=0,1,2$. Notice that we have made use of the quantities ω_l^0 and ω_A^0 defined in (83) and of the quantities $\alpha_0(M_F,x)$ and $\alpha_1(M_F,x)$ defined in (49). Here and in the following $M_F=F_-$ if $j_1=F_-,F_-$ and $M_F=-F_-$ if $j_1=F_-,-F_-$.

Using (90)–(92) one finds that (87) reduces to

$$i\frac{\partial}{\partial\tau}\begin{pmatrix}\phi_{j_0}^0(x,\tau)\\\phi_{j_2}^0(x,\tau)\\\phi_{j_1}^0(x,\tau)\end{pmatrix}=[\mathbb{M}_0(x,\tau)+\epsilon\mathbb{M}_1(x,\tau)]\begin{pmatrix}\phi_{j_0}^0(x,\tau)\\\phi_{j_2}^0(x,\tau)\\\phi_{j_1}^0(x,\tau)\end{pmatrix}.\tag{93}$$

When we defined $\phi_{j_l}^0(x,\tau)$ in (91) we eliminated the fast (time) evolution of $\phi_{j_l}(x,\tau)$ if the atom is well localized around $\zeta_R(\tau_0)/\kappa$. This fast evolution is associated with the internal and gravitational potential energies. All that is left is the slow (time) evolution due to the interaction with $\mathbf{B}_p(t)$ and due to the coupling $\mathbb{L}^0(x)$ introduced by the use of the position-dependent basis Γ. Hence, we assume that the $\phi_{j_l}^0(x,\tau)$ $(l=0,1,2)$ evolve on a time scale much larger than π/ω_A^0 and $2\pi/(\omega_2^0-\omega_1^0)$; that

is, we assume that

$$\phi^0_{j_l}(x,\tau') \simeq \phi^0_{j_l}(x,\tau) \quad (l=0,1,2), \tag{94}$$

if $\tau,\tau' \in (\tau_0,\tau_1)$ and

$$|\tau'-\tau| \leqslant \frac{\pi}{\omega^0_A}, \frac{2\pi}{(\omega^0_2-\omega^0_1)}. \tag{95}$$

Therefore, one can perform the RWA in (93); that is, one can neglect terms in (93) that average to zero because they oscillate at (angular) frequencies of $2\omega^0_A$ and $(\omega^0_2-\omega^0_1)$. One obtains exactly the same equation as in (93) with the change

$$[\mathbb{M}_0(x,\tau)+\epsilon\mathbb{M}_1(x,\tau)] \to [\mathbb{M}'_0(x)+\epsilon\mathbb{M}'_1(x)]. \tag{96}$$

Here we have introduced the matrices

$$\begin{aligned}
\mathbb{M}'_0(x) &= \begin{pmatrix} \mathbb{M}_{00}(x) & 0 & \Omega_0(x) \\ 0 & \mathbb{M}_{22}(x) & 0 \\ \Omega_0(x)^* & 0 & \mathbb{M}_{11}(x) \end{pmatrix}, \\
\mathbb{M}'_1(x) &= \begin{pmatrix} -\frac{\partial^2}{\partial x^2} & 0 & 0 \\ 0 & \mathbb{N}_{22}(x,M_F) & 0 \\ 0 & 0 & \mathbb{N}_{22}(x,M_F) \end{pmatrix}.
\end{aligned} \tag{97}$$

The validity of the RWA is discussed in a section below.

Notice that the matrix on the right side of (96) is now time independent. Moreover, the coupling between $\phi^0_{j_2}(x,\tau)$ and $\phi^0_{j_1}(x,\tau)$ disappeared with the RWA. Hence, it follows from (93), (96), and the initial conditions in (88) that

$$\phi^0_{j_2}(x,\tau) = 0; \tag{98}$$

that is, this wave function is zero because it started out as zero and it is not coupled to $\phi^0_{j_l}(x,\tau)$ for $l=0,1$.

From (93)–(98) it follows that we are left with a two-level problem that can be written as

$$i\frac{\partial}{\partial\tau}\begin{pmatrix}\phi^0_{j_0}(x,\tau)\\ \phi^0_{j_1}(x,\tau)\end{pmatrix} = [\mathbb{M}''_0(x)+\epsilon\mathbb{M}''_1(x)]\begin{pmatrix}\phi^0_{j_0}(x,\tau)\\ \phi^0_{j_1}(x,\tau)\end{pmatrix}, \tag{99}$$

with

$$\mathbb{M}''_0(x) = \begin{pmatrix} V^0_{j_0}(x)-\omega^0_0+\frac{Mg_0}{\hbar\Delta W\kappa}x & \Omega_0(x) \\ \Omega_0(x)^* & V^0_{j_1}(x)-\omega^0_1+\frac{Mg_0}{\hbar\Delta W\kappa}x \end{pmatrix}, \tag{100}$$

and

$$\mathbb{M}''_1(x) = \begin{pmatrix} -\frac{\partial^2}{\partial x^2} & 0 \\ 0 & -\frac{\partial^2}{\partial x^2}-\alpha_0(M_F,x) \end{pmatrix}. \tag{101}$$

We now take advantage of the fact that $\epsilon \ll 1$ to use perturbation theory to solve (99).

Assume that the solution of (99) has the asymptotic expansion

$$\begin{pmatrix}\phi^0_{j_0}(x,\tau)\\ \phi^0_{j_1}(x,\tau)\end{pmatrix} \sim \begin{pmatrix}\phi^0_{00}(x,\tau)\\ \phi^0_{10}(x,\tau)\end{pmatrix} + \epsilon\begin{pmatrix}\phi^0_{01}(x,\tau)\\ \phi^0_{11}(x,\tau)\end{pmatrix} + \cdots. \tag{102}$$

Substituting (102) in (99) one finds the following set of equations:

$$\begin{aligned}
i\frac{\partial}{\partial\tau}\begin{pmatrix}\phi^0_{00}(x,\tau)\\ \phi^0_{10}(x,\tau)\end{pmatrix} &= \mathbb{M}''_0(x)\begin{pmatrix}\phi^0_{00}(x,\tau)\\ \phi^0_{10}(x,\tau)\end{pmatrix}, \\
i\frac{\partial}{\partial\tau}\begin{pmatrix}\phi^0_{0l}(x,\tau)\\ \phi^0_{1l}(x,\tau)\end{pmatrix} &= \mathbb{M}''_0(x)\begin{pmatrix}\phi^0_{0l}(x,\tau)\\ \phi^0_{1l}(x,\tau)\end{pmatrix} \\
&\quad + \mathbb{M}''_1(x)\begin{pmatrix}\phi^0_{0,l-1}(x,\tau)\\ \phi^0_{1,l-1}(x,\tau)\end{pmatrix},
\end{aligned} \tag{103}$$

for each $l=1,2,\ldots$. From (88) and (102) one finds that these equations are subject to the initial conditions

$$\begin{aligned}
\begin{pmatrix}\phi^0_{00}(x,\tau_0)\\ \phi^0_{10}(x,\tau_0)\end{pmatrix} &= \begin{pmatrix}\phi(x,\tau_0)\\ 0\end{pmatrix}, \\
\begin{pmatrix}\phi^0_{0l}(x,\tau_0)\\ \phi^0_{1l}(x,\tau_0)\end{pmatrix} &= \begin{pmatrix}0\\ 0\end{pmatrix}
\end{aligned} \tag{104}$$

for each $l=1,2,\ldots$. Although $\phi(x,\tau_0)$ does depend on ϵ, the initial conditions in (104) remain valid because we are only using ϵ to determine the form of $\phi(x,\tau_0)$ and not to alter the order established in (102).

The equations in (103) subject to the initial conditions in (104) are solved using the exponential of a matrix [25]. It can be shown that $\exp[i\mathbb{M}''_0(x)(\tau-\tau_0)]$ is a 2×2 unitary matrix given by

$$\begin{aligned}
&\exp[i\mathbb{M}''_0(x)(\tau-\tau_0)] \\
&\quad = e^{i\Omega_p(x)(\tau-\tau_0)}\begin{pmatrix}\mathbb{U}_{11}(x,\tau) & -\mathbb{U}_{21}(x,\tau)\\ \mathbb{U}_{21}(x,\tau) & \mathbb{U}_{11}(x,\tau)^*\end{pmatrix},
\end{aligned} \tag{105}$$

with the quantities defined in (82).

Using (105) it follows for $l=1,2,\ldots$ that

$$\begin{aligned}
\begin{pmatrix}\phi^0_{00}(x,\tau)\\ \phi^0_{10}(x,\tau)\end{pmatrix} &= \exp[-i\mathbb{M}''_0(x)(\tau-\tau_0)]\begin{pmatrix}\phi(x,\tau_0)\\ 0\end{pmatrix} \\
&= \phi(x,\tau_0)e^{-i\Omega_p(x)(\tau-\tau_0)}\begin{pmatrix}\mathbb{U}_{11}(x,\tau)^*\\ -\mathbb{U}_{21}(x,\tau)\end{pmatrix}, \\
\begin{pmatrix}\phi^0_{0l}(x,\tau)\\ \phi^0_{1l}(x,\tau)\end{pmatrix} &= -i\exp\left[-i\mathbb{M}''_0(x)(\tau-\tau_0)\right] \\
&\quad \times \int_{\tau_0}^{\tau} d\tau' \exp[i\mathbb{M}''_0(x)(\tau'-\tau_0)] \\
&\quad \times \mathbb{M}''_1(x)\begin{pmatrix}\phi^0_{0(l-1)}(x,\tau')\\ \phi^0_{1(l-1)}(x,\tau')\end{pmatrix}.
\end{aligned} \tag{106}$$

The results in the second line of (106) are expressed in a simple form that can be evaluated numerically, but only the first-term approximation [the first line in (106)] provides an explicit analytic form that can be handled with ease.

In the following we restrict to a first-term approximation of the exact solution of (99) with the initial conditions in (104). Moreover, we assume that it provides an accurate description of the exact solution. Its accuracy is discussed in the following

section. The state of the system at time $t = \tau/\Delta W \in (t_0,t_1)$ is then given by (80) and (81).

B. Accuracy of the first-term approximation

In this section we establish a criterion that can be evaluated numerically to determine whether the first-term approximation in (81) is accurate. Moreover, we discuss the conditions under which one should expect the approximation to work.

From (102) we know that a two-term approximation is given by

$$\begin{aligned}\begin{pmatrix}\phi^0_{j_0}(x,\tau)\\ \phi^0_{j_1}(x,\tau)\end{pmatrix} &\sim \begin{pmatrix}\phi^0_{00}(x,\tau)\\ \phi^0_{10}(x,\tau)\end{pmatrix} + \epsilon\begin{pmatrix}\phi^0_{01}(x,\tau)\\ \phi^0_{11}(x,\tau)\end{pmatrix}\\ &= e^{-i\mathbb{M}''_0(x)(\tau-\tau_0)}\left[\begin{pmatrix}\phi(x,\tau_0)\\ 0\end{pmatrix}\right.\\ &\quad \left. - i\epsilon\int_{\tau_0}^{\tau} d\tau' e^{i\mathbb{M}''_0(x)(\tau'-\tau_0)}\mathbb{M}''_1(x)\begin{pmatrix}\phi^0_{00}(x,\tau')\\ \phi^0_{10}(x,\tau')\end{pmatrix}\right],\end{aligned} \tag{107}$$

with $x \in \mathbb{R}$ and $\tau \in (\tau_0,\tau_1)$. Hence, the first-term approximation will be accurate if

$$\epsilon\left|\int_{\tau_0}^{\tau} d\tau' f_k(x,\tau')\right| \ll \begin{cases}|\phi(x,\tau_0)| & \text{if} \quad k=1,\\ 1 & \text{if} \quad k=2,\end{cases} \tag{108}$$

for each x, where $|\phi(x,\tau_0)|$ has non-negligible values and $\tau \in [\tau_0,\tau_1)$. Here

$$\mathbf{f}(x,\tau') = \exp[i\mathbb{M}''_0(x)(\tau'-\tau_0)]\mathbb{M}''_1(x)\begin{pmatrix}\phi^0_{00}(x,\tau')\\ \phi^0_{10}(x,\tau')\end{pmatrix}, \tag{109}$$

and $f_k(x,\tau')$ denotes the kth component of $\mathbf{f}(x,\tau')$.

Using the property that the modulus of an integral is less than or equal to the integral of the modulus, it follows from (108) that the first-term approximation will be accurate if

$$\epsilon\int_{\tau_0}^{\tau_1} d\tau'|f_k(x,\tau')| \ll \begin{cases}|\phi(x,\tau_0)| & \text{if} \quad k=1,\\ 1 & \text{if} \quad k=2,\end{cases} \tag{110}$$

for each x where $|\phi(x,\tau_0)|$ has non-negligible values. In this article we use (110) to determine whether the first-term approximation is accurate.

It is important to realize that the first-term approximation is always accurate if the duration $(\tau_1-\tau_0)$ of the pulse is sufficiently small. In particular, from (86) we know that a necessary condition for the first-term approximation to be accurate is that the atom must move a negligible distance during the application of the pulse. Nevertheless, our numerical calculations indicate that this is not a sufficient condition (the reason for this is that other position-dependent quantities such as the phase of the wave function also play a role). To find if $(\tau_1-\tau_0)$ is sufficiently small one has to evaluate (110) numerically. Since (110) appears to give no clue as to when one should expect the first-term approximation to be accurate, we now derive an estimate that does give some insight.

First observe that

$$\epsilon\int_{\tau_0}^{\tau_1} d\tau'|f_k(x,\tau')| \leqslant \epsilon(\tau_1-\tau_0)||\mathcal{A}||, \tag{111}$$

with

$$\mathcal{A} \equiv \mathbb{M}''_1(x)\begin{pmatrix}\phi^0_{00}(x,\tau'')\\ \phi^0_{10}(x,\tau'')\end{pmatrix}, \tag{112}$$

$\tau'' \in [\tau_0,\tau_1]$, $k = 1,2$, and $||\cdot||$ the usual Euclidean vector norm. To obtain (111) we used the mean value theorem for integrals, the Cauchy-Schwarz inequality, and the fact that $\exp[i\mathbb{M}''_0(x)(\tau-\tau_0)]$ is a unitary matrix.

We now bound $||\mathcal{A}||$. First observe from (70) that

$$\begin{aligned}\frac{\partial}{\partial x}\phi(x,\tau) &= f_1(x,\tau)\phi(x,\tau),\\ \frac{\partial^2}{\partial x^2}\phi(x,\tau) &= [f_1(x,\tau)^2 + f_2(x,\tau)]\phi(x,\tau),\end{aligned} \tag{113}$$

where $t = \tau/\Delta W \in [0,t_0]$, $x \in \mathbb{R}$, and

$$\begin{aligned}f_1(x,\tau) &= i\frac{\langle P_z\rangle(t)}{\hbar\kappa} - \frac{x-\zeta(\tau)}{2[\sigma_x(0)^2 + i\epsilon\tau]},\\ f_2(x,\tau) &= -\frac{1}{2[\sigma_x(0)^2 + i\epsilon\tau]}.\end{aligned} \tag{114}$$

Now we make the following approximations.

(1) Neglect $\alpha_0(M_F,x)$.

(2) Neglect the first and second derivatives with respect to x of $\Omega_p(x)$, $\Omega_R(x)$, and $\Theta_R(x)$.

(3) Take $x = \zeta(\tau_0)$.

Making these approximations and using (113) it is straightforward to show that

$$\begin{aligned}||\mathcal{A}|| \simeq [2\pi\kappa^2\Delta Z(t_0)^2]^{-1/4}\left|\left[\frac{\langle P_z\rangle(t_0)}{\hbar\kappa}\right]^2 + \frac{1}{2\kappa^2\Delta Z(t_0)^2}\right.\\ \left. - i\frac{\epsilon\Delta W t_0}{2\kappa^4\Delta Z(0)^2\Delta Z(t_0)^2}\right|.\end{aligned} \tag{115}$$

It follows form (110) and (111) that the first-term approximation will be accurate if the right side of (111) with (115) is much smaller than 1 and $|\phi(x,\tau_0)|$ for each x where $|\phi(x,\tau_0)|$ has non-negligible values (assuming that the three approximations above are valid). Our numerical calculations show that it is a rough estimate and, therefore, it should be taken only as an expression that gives insight into the conditions that have to be met so that the first-term approximation is accurate.

We now relate the aforementioned estimate to the (nondimensional) Rabi frequency $\Omega_R(x)$. In order to do this, lets take τ_1 to be given by

$$\tau_1 = \frac{\pi}{\Omega_R[\zeta_R(\tau_0)]} + \tau_0, \tag{116}$$

so that we have a π pulse. From (115) and (116) it follows that

$$\begin{aligned}\epsilon(\tau_1-\tau_0)||\mathcal{A}|| \simeq \frac{\epsilon\pi}{\Omega_R[\zeta_R(\tau_0)]}[2\pi\kappa^2\Delta Z(t_0)^2]^{-1/4}\left|\left[\frac{\langle P_z\rangle(t_0)}{\hbar\kappa}\right]^2\right.\\ \left. + \frac{1}{2\kappa^2\Delta Z(t_0)^2} - i\frac{\epsilon\Delta W t_0}{2\kappa^4\Delta Z(0)^2\Delta Z(t_0)^2}\right|.\end{aligned} \tag{117}$$

Since one requires $\epsilon(\tau_1-\tau_0)||\mathcal{A}|| \ll 1$, from (117) we find that larger values of $\langle P_z\rangle(t_0)$ require larger values of the Rabi frequency $\Omega_R[\zeta_R(\tau_0)]$ and, hence, of B_0. Moreover, it is clear that $\langle P_z\rangle(t_0) \simeq 0$ will allow one to use the smallest values of $\Omega_R[\zeta_R(\tau_0)]$. Our numerical calculations led us also to these conclusions and they are in accordance with the condition that the atom must move a negligible distance during the application of the pulse.

Finally, we emphasize that it is important to establish if the first-term approximation is accurate or not, since the validity of the results rely on this. Moreover, it is also important in the interpretation of experiments because the instant in which the pulse is applied might imply large values of B_0 for the first-term approximation to be accurate and these might not be used or the equipment available might not even be able to reach them. Hence, more terms in the asymptotic expansion would have to be included in order to explain correctly the results of the experiment.

C. Validity of the RWA

Recall that (99) was derived from (93) using the RWA and (98) (the latter being a consequence of the RWA and the initial conditions). Moreover, the RWA is valid if and only if the conditions in (94) and (95) are satisfied. In this section we express them in terms of the position-dependent (nondimensional) Rabi frequency $\Omega_R(x)$.

First assume that the first-term approximation provides an accurate description of the exact solution of (99) for $\tau \in (\tau_0,\tau_1)$ with the initial conditions in (88). Then it follows from (94), (95), and (106) that the RWA is valid if and only if

$$|\Omega_p(x)|, \quad \tfrac{1}{2}\Omega_R(x) \ll 2\omega_A^0,\omega_2^0-\omega_1^0, \tag{118}$$

for each x where $|\phi(x,\tau_0)|$ has non-negligible values. If in addition $\phi(x,\tau_0)$ is well localized around $x=\zeta_R(\tau_0)$ [that is, the atom is well localized around $\zeta_R(\tau_0)/\kappa$ at time t_0], then $\Omega_p(x)$ is approximately zero and $\Omega_R(x)$ can be evaluated at $x=\zeta_R(\tau_0)$. In this case the RWA is valid if and only if

$$\tfrac{1}{2}\Omega_R[\zeta_R(\tau_0)] \ll 2\omega_A^0,\omega_2^0-\omega_1^0. \tag{119}$$

Hence, one recovers the condition for the validity of the RWA corresponding to the case of a two-level atom fixed at a position and interacting resonantly with an electric (magnetic) field [26].

We now make some comments on how the RWA can break down. Recall that in the first-term approximation the atom moves a negligible distance during the application of the pulse $\mathbf{B}_p(t)$. Also, in (91) we eliminated the fast free evolution of $\phi_{j_l}(x,\tau)$ in $\phi_{j_l}^0(x,\tau)$ when the atom is fixed at $\zeta_R(\tau_0)/\kappa$. If the atom moves a non-negligible distance, then the fast free evolution of $\phi_{j_l}(x,\tau)$ will change and it will not be completely eliminated in $\phi_{j_l}^0(x,\tau)$. In fact, this fast free evolution of $\phi_{j_l}(x,\tau)$ at the new positions can be very different from that at $\zeta_R(\tau_0)$. Hence, the RWA gets progressively worse and it can eventually break down if the atom moves a non-negligible distance during the application of $\mathbf{B}_p(t)$. We had already observed in the paragraph following (28) that the model is not valid if the duration of the pulse is sufficiently long. Finally, one cannot simply change the transformation defining $\phi_{j_l}^0(x,\tau)$ so as to eliminate the fast free evolution of $\phi_{j_l}(x,\tau)$ at another position, since this would require that the frequency ω_A of $\mathbf{B}_p(t)$ to change as the atom moves. Moreover, it is not entirely clear how ω_A would have to change in time, since one can see from (99) that components of the state of the atom move under different potentials.

D. Probability to make the transition

In this subsection we determine the probability $P(t)$ for the atom to make the transition, that is, the probability to find the atom at time $t \in (t_0,t_1)$ in the set of states

$$\{|z,V_{j_1}[x(z)]\rangle : z \in \mathbb{R}\}. \tag{120}$$

From (80)–(82) one finds that

$$\begin{aligned} P(t) &= \int_{-\infty}^{+\infty} dx\,|\phi_{j_1}(x,\tau)|^2, \\ &\simeq \int_{-\infty}^{+\infty} dx\,|\phi(x,\tau_0)|^2 \sin^2[\Theta_R(x)]\sin^2\left[\frac{\Omega_R(x)}{2}(\tau-\tau_0)\right], \end{aligned} \tag{121}$$

with $t=\tau/\Delta W$. Notice that (121) is the usual formula for Rabi oscillations in the Jaynes-Cummings model [26] averaged by the (nondimensional) position pdf $|\phi(x,\tau_0)|^2$ of the atom at the beginning of the pulse [see (86)]. We mention that the two-term approximation does include the velocity of the atom since $\phi_{11}^0(x,\tau)$ in (106) depends on the first and second partial derivatives of $\phi(x,\tau)$ with respect to x and these depend on $\langle P_z\rangle(t)$ [see (113) and (114)].

From (121) one observes that the wave packet $\phi(x,\tau_0)$ can alter considerably the probability of the transition. Suppose first that the atom is well localized around $\langle Z\rangle(t_0)=\zeta(\tau_0)/\kappa$ at the beginning of the pulse $\mathbf{B}_p(t)$; that is, $\Delta Z(t_0)=\sigma_x(\tau_0)/\kappa$ is sufficiently small so that $|\phi(x,\tau_0)|^2$ is well localized around $\zeta(t_0)$. Then (121) takes the well-known form describing Rabi oscillations

$$P(t) \simeq \sin^2\{\Theta_R[\zeta(\tau_0)]\}\sin^2\left\{\frac{\Omega_R[\zeta(\tau_0)]}{2}(\tau-\tau_0)\right\}. \tag{122}$$

If one wishes to apply a π pulse, that is, if one wishes to apply a pulse that sends the atom to the set of states in (120), then τ_1 has to be chosen as in (116). Using that $|\phi(x,\tau_0)|^2$ is well localized around $\zeta(\tau_0)=\zeta_R(\tau_0)$ and assuming that $i\Omega_0[\zeta(\tau_0)]>0$ (see the paragraph following (84) for sufficient conditions for this to hold), it follows from (80)–(83), (85), and (122) that $P(t_1)\simeq 1$ and

$$|\psi(t_1)\rangle \simeq e^{-i\theta_\pi}\int_{-\infty}^{+\infty} dx\,\frac{1}{\sqrt{\kappa}}\left|\frac{x}{\kappa},V_{j_1}(x)\right\rangle\phi(x,\tau_0), \tag{123}$$

with $\theta_\pi=\omega_1^0\pi/\Omega_R[\zeta_R(\tau_0)]$. Comparing (123) with the state of the system at the beginning of the pulse, that is, with (73) at time $t=t_0=\tau_0/\Delta W$, we observe that (except for a global phase) the effect of the π pulse is simply to change the internal state of the atom (j_0 changes to j_1). Recall that this is precisely what we described as a pulse in preceding paragraphs.

Now suppose that the atom is not well localized at the beginning of the pulse and that one wishes to apply a π pulse.

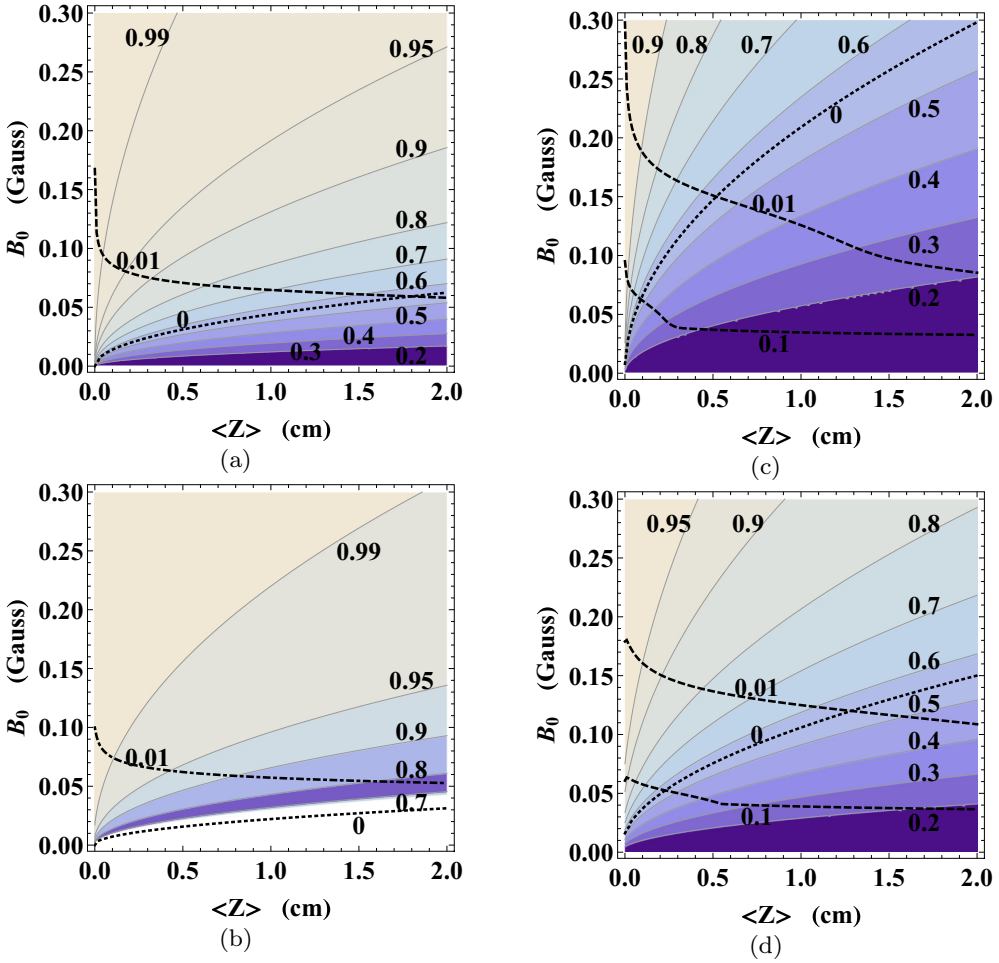

FIG. 1. (Color online) The figures show contour plots of the probability $P(t_1)$ that the atom makes the transition at the end of a π pulse (purple solid lines), the criterion for the accuracy of the first-term approximation (black dashed lines), and the criterion that the atom makes the transition (black dotted line with value 0) as a function of the maximum height $\langle Z\rangle$ and B_0. The π pulse is applied from $t = t_0$ to $t = t_1$, with t_0 the instant in which the atom reaches the maximum height $\langle Z\rangle$ starting from $z = 0$ at $t = 0$. Panels (a) and (b) ((c) and (d)) have $\eta = 10$ (100) G/cm. Also, (a) and (c) ((b) and (d)) have $\Delta Z(0) = 5 \times 10^{-7}$ (10^{-6}) m.

Then the probability of transition $P(t_1)$ in (121) diminishes greatly. These facts are illustrated further below in Fig. 1, but we first propose a criterion to determine whether the atom makes the transition or not due to the width of the wave packet $\phi(x,\tau)$ in the case $\zeta(\tau_0) = \zeta_R(\tau_0)$ or, equivalently, in the case were the expected value of the position of the atom $\langle Z\rangle(\tau_0)$ at time t_0 is equal to the *resonant position* $\zeta_R(\tau_0)/\kappa$. Recall that this position is *resonant* because the angular frequency ω_A of $\mathbf{B}_p(t)$ was chosen to be equal to the angular transition frequency when the atom is exactly located at $\zeta_R(\tau_0)/\kappa$ [see the paragraphs following (83)].

Observing (121) we propose the following criterion: The transition does not take place if

$$\sin^2[\Theta_R(y)]|_{y=y_\pm\equiv\zeta_R(\tau_0)\pm\sigma_x(\tau_0)} \leqslant \tfrac{1}{2}. \qquad (124)$$

Recall that $\sigma_x(\tau)$ is the nondimensional standard deviation in position [see its definition in (74)]. We note that the transition does not take place if the inequality in (124) is satisfied for at least one of $y_\pm$. In simple terms the proposed criterion states that the transition does not take place at the end of the π pulse if the half width at half maximum (HWHM) of $\sin^2[\Theta_R(x)]$ is smaller than the HWHM of $|\phi(x,\tau_0)|^2$. The criterion in (124) has the purpose of identifying when an atom that would make the transition if it were well localized [that is, if the atom were well localized around the *resonant position* $\zeta_R(t_0)/\kappa$], actually does make the transition at least half the times due to the expansion of the wave packet. We chose the value $1/2$ as the border of making the transition or not at the end of the π pulse because it is the most relaxed condition one can impose (half the times the atom makes the transition).

We now simplify the criterion in (124). Using the definition of $\Theta_R(y)$ in (83), it follows that (124) is equivalent to $\delta_{00}(y_\pm)^2 - 4|\Omega_0(y_\pm)|^2 \geqslant 0$. Using Taylor series centered at $\zeta_R(\tau_0)$ and neglecting terms of order $[x - \zeta_R(\tau_0)]^n$ with $n \geqslant 3$, it follows that

$$\delta_{00}(x)^2 - 4|\Omega_0(x)|^2 \simeq a_0(y_0)[x - \zeta_R(\tau_0) - r_+(y_0)] \times [x - \zeta_R(\tau_0) - r_-(y_0)], \qquad (125)$$

with $y_0 = \zeta_R(\tau_0)$ and

$$r_{\pm}(y) = \frac{2}{a_0(y)}\left\{\frac{d}{dy}|\Omega_0(y)|^2 \pm \sqrt{\left[\frac{d}{dy}|\Omega_0(y)|^2\right]^2 + a_0(y)|\Omega_0(y)|^2}\right\}, \quad (126)$$

$$a_0(y) = \left[\frac{d}{dy}\delta_{00}(y)\right]^2 - 2\left[\frac{d^2}{dy^2}|\Omega_0(y)|^2\right].$$

Moreover, the right side of (125) will be an accurate approximation of the left side if

$$\begin{aligned} &\left[\frac{d}{dy}\delta_{00}(y)\Big|_{y=\zeta_R(\tau_0)}\right]^2 \\ &\quad \gg \left|\frac{d^3}{dy^3}\delta_{00}(y)^2\Big|_{y=\zeta_R(\tau_0)}\right|\left|\frac{1}{3!}|x-\zeta_R(\tau_0)|,\right. \\ &\left|\frac{d^2}{dy^2}|\Omega_0(y)|^2\Big|_{y=\zeta_R(\tau_0)}\right| \\ &\quad \gg \left|\frac{d^3}{dy^3}|\Omega_0(y)|^2\Big|_{y=\zeta_R(\tau_0)}\right|\left|\frac{1}{3}|x-\zeta_R(\tau_0)|.\right. \end{aligned} \quad (127)$$

These conditions are deduced by asking that the correction of order $[x-\zeta_R(\tau_0)]^3$ to the right side of (125) be much smaller than the right side of (125).

Using (125) and the definitions in (83) one can conclude that if $a_0[\zeta_R(\tau_0)] > 0$ and (127) are satisfied for $x = y_{\pm} = \zeta_R(\tau_0) \pm \sigma_x(\tau_0)$, then (124) is equivalent to

$$\tau_0 - \frac{\sigma_x(0)}{\epsilon}\sqrt{\max\{0, r_{\pm}[\zeta_R(\tau_0)]^2 - \sigma_x(0)^2\}} \geqslant 0. \quad (128)$$

That is, the transition does no take place if (128) is satisfied. We mention that one should expect the conditions in (127) to be satisfied for $x = y_{\pm} = \zeta_R(\tau_0) \pm \sigma_x(\tau_0)$ since the functions $\delta_{00}(x)$ and $|\Omega_0(x)|$ normally do not vary much over the extension of $|\phi(x,\tau_0)|^2$. Also notice that (128) is a very simple criterion that can be used to determine whether the transition will take place.

We now illustrate the above results concerning $P(t)$. Consider a ^{87}Rb atom, $j_0 = F_+, F_+ = 2,2$, and $j_1 = F_-, F_- = 1,1$. The atom has the initial state given in (68), (69), and (72) with $\zeta(\tau_0) = \zeta_R(\tau_0)$, expected value of position $z_0 = 0$ at time $t = 0$, and expected value of momentum p_0 at time $t = 0$ such that the expected value of the position of the atom reaches a maximum height $\langle Z\rangle$. At the instant $t = t_0$ in which the atom reaches the maximum height $\langle Z\rangle$, the magnetic field $\mathbf{B}_p(t)$ is applied from $t = t_0$ to $t = t_1 = \tau_1/\Delta W$. The probability $P(t)$ that the atom makes the transition is calculated numerically using the second line in (121). Notice that $\zeta(\tau_0) = \zeta_R(\tau_0)$ was chosen so that $\mathbf{B}_p(t)$ is resonant with the transition if the atom is well localized around its expected value of position $\zeta(t_0)/\kappa$ at time $t = t_0$.

First consider a π pulse, that is, τ_1 given in (116). Figure 1 shows contour plots of $P(t = t_1)$ for different values of the maximum height $\langle Z\rangle$, the strength B_0 of $\mathbf{B}_p(t)$, the standard deviation of position $\Delta Z(0)$ at time $t = 0$, and the derivative η of $B_{\rm ST}(z)$. Figures 1(a) and 1(b) have $\eta = 10$ G/cm, while Figs. 1(c) and 1(d) have $\eta = 100$ G/cm. Moreover, Figs. 1(a) and 1(c) have $\Delta Z(0) = 5\times 10^{-7}$ m, while Figs. 1(b) and 1(d) have $\Delta Z(0) = 10^{-6}$ m.

In Fig. 1 the contours 0.01 and 0.1 limit the region in which the first-term approximation is known to be accurate. In the region above the yth contour ($y = 0.01, 0.1$), the two-term approximation can modify the first-term approximation at most in $y\times 10^2\%$ so that the first-term approximation is accurate. We now describe how these contours were obtained. The integrals in (110) where evaluated numerically in an 11-point uniform mesh from $x = \zeta(\tau_0) - 5\sigma_x(\tau_0)$ to $x = \zeta(\tau_0) + 5\sigma_x(\tau_0)$ and the maximum value was taken. This was done for each value of $\zeta(\tau_0) = \kappa\langle Z\rangle$ in a uniform mesh between $\langle Z\rangle = 0$ cm and $\langle Z\rangle = 2$ cm. The values of the integrals associated with the first components of (110) were divided by $|\phi[\zeta(\tau_0),\tau_0]|$ (the maximum value of $|\phi(x,\tau_0)|$). Then the maximums between the latter (values of the first components of the integrals divided by $|\phi[\zeta(\tau_0),\tau_0]|$) and the integrals associated with the second components of (110) were taken to construct the contours.

The contour 0 of the function on the left of (128) is also shown. Hence, according to the criterion in (128), the transition only takes place in the region above this contour. One observes from Fig. 1 that the criterion works very well, since the region above the 0 contour has $P(t_1) > 1/2$.

From Fig. 1 one notices that the uncertainty in position $\Delta Z(t)$ of the atom has a deteriorating effect on $P(t_1)$. It can be observed in Figs. 1(a) and 1(c) that $P(t_1)$ decreases very rapidly for increasing maximum height $\langle Z\rangle$ when compared to Figs. 1(b) and 1(d). The reason for this is that $\Delta Z(t)$ grows more rapidly when $\Delta Z(0) = 5\times 10^{-7}$ m when compared to the case where $\Delta Z(0) = 10^{-6}$ m [see the formula for $\Delta Z(t)$ in (74)]. Notice that $P(t_1)$ decreases considerably because $\mathbf{B}_p(t)$ is not resonant with the desired transition when the atom is not well localized. Moreover, one also observes that the uncertainty in position $\Delta Z(t)$ of the atom has a more deteriorating effect for larger η. The reason for this is that the nondimensional uncertainty $\sigma_x(\tau)$ is larger for larger η; that is, in a sense, the expansion of the wave packet is more noticeable for larger η.

Also notice in Fig. 1 that $P(t_1)$ increases with larger B_0. To explain this fact, first observe from (55) that the atom-$\mathbf{B}_p(t)$ coupling $\Omega_0(x)$ increases with larger B_0. Hence, it follows from the definitions in (83) that the (nondimensional) Rabi frequency $\Omega_R(x)$ increases with B_0, while the (nondimensional) detuning $\delta_{00}(x)$ is independent of B_0. Using the continuity of the function $\delta_{00}(x)/\Omega_R(x)$ and the fact that $\delta_{00}[\zeta_R(\tau_0)] = 0$ [see (85)], it follows that the length of the interval $\mathcal{I}_\delta$ centered at $\zeta_R(\tau_0)$ and in which $\delta_{00}(x)/\Omega_R(x) \simeq 0$ increases with larger B_0. Since $\Omega_R(x)$ varies slowly with x and $\sin^2[\Theta_R(x)] \simeq 1$ for $x \in \mathcal{I}_\delta$ [see the definition of $\Theta_R(x)$ in (83)], one concludes from (121) that $P(t_1)$ increases with larger B_0. Also, as the length of $\mathcal{I}_\delta$ grows it includes more and more of the region $\mathcal{I}_\phi$ where $|\phi(x,\tau_0)|^2$ takes non-negligible values. For sufficiently large B_0 the interval $\mathcal{I}_\delta$ contains $\mathcal{I}_\phi$ and $|\phi(x,\tau_0)|^2$ can be considered to be well localized. In this case (122) applies and one obtains from (116) that $P(t_1) \simeq 1$ when $\zeta_R(\tau_0) = \zeta(\tau_0)$. In simple terms, $P(t_1)$ increases with larger values of B_0 because the atom-$\mathbf{B}_p(t)$ interaction becomes less sensitive to the position of the atom.

Finally, consider a 2π pulse, that is, τ_1 is chosen as

$$\tau_1 = \frac{2\pi}{\Omega_R[\zeta_R(\tau_0)]} + \tau_0. \tag{129}$$

Figure 2 illustrates $P(t = \tau/\Delta W)$ as a function of $\tau \in [\tau_0, \tau_1]$ for $B_0 = 0.3$ G and several values of the maximum height $\langle Z\rangle$. Figures 2(a) and 2(c) have $\Delta Z(0) = 5 \times 10^{-7}$ m, while Figs. 2(b) and 2(d) have $\Delta Z(0) = 10^{-6}$ m. Also, Figs. 2(a) and 2(b) have $\eta = 10$ G/cm, while Figs. 2(c) and 2(d) have $\eta = 100$ G/cm. Notice that the uncertainty in position $\Delta Z(t)$ of the atom leads to a deteriorating visibility of the Rabi oscillation for increasing $\langle Z\rangle$. This is particularly noticeable for smaller values of $\Delta Z(0)$ and larger values of η, since $\Delta Z(t)$ increases faster in the first case and the expansion of the wave packet is more noticeable in the second [$\sigma_x(\tau)$ is larger for larger η].

VI. THE PHASE-SPACE SELECTOR

We now use the results obtained so far to characterize the phase-space selector presented in the Introduction. In the rest of this section we assume that the first-term approximation is accurate, the atom is well localized around its expected value of position $\langle Z\rangle(t_0) = \zeta(\tau_0)/\kappa$ at time $t_0 = \tau_0/\Delta W$, a π pulse is applied with τ_1 in (116), $a_0[\zeta_R(\tau_0)] > 0$, and conditions (127) hold with $x = \zeta(\tau_0)$.

Define the interval

$$I_S[\zeta_R(\tau_0)] = [l_-[\zeta_R(\tau_0)], l_+[\zeta_R(\tau_0)]] \tag{130}$$

with

$$l_\pm[\zeta_R(\tau_0)] = \frac{\zeta_R(\tau_0) + r_\pm[\zeta_R(\tau_0)]}{\kappa}. \tag{131}$$

Recall that $r_\pm(y)$ was defined in (126).

Since the first-term approximation is accurate and the atom is well localized around its expected value of position $\langle Z\rangle(t_0) = \zeta(\tau_0)/\kappa$ at time $t_0 = \tau_0/\Delta W$, one can use expression (122) with $t = t_1$ for the probability $P(t_1)$ to find the atom in the set of states (120) at time t_1. Using that expression and the definition of $\Theta_R(x)$ in (83), one obtains the following implications:

$$\begin{aligned} 0 \;&<\; \delta_{00}(x)^2 - 4|\Omega_0(x)|^2|_{x=\zeta(\tau_0)} \\ &\Leftrightarrow\; \sin^2[\theta_R(x)]|_{x=\zeta(\tau_0)} < \tfrac{1}{2} \\ &\Rightarrow\; P(t_1) < \tfrac{1}{2}. \end{aligned} \tag{132}$$

Since $a_0[\zeta_R(\tau_0)] > 0$ and conditions (127) hold with $x = \zeta(\tau_0)$, one can use (125) to conclude that

$$\langle Z\rangle(t_0) \notin I_S[\zeta_R(\tau_0)] \Rightarrow 0 < \delta_{00}(x)^2 - 4|\Omega_0(x)|^2|_{x=\zeta(\tau_0)}. \tag{133}$$

Combining (132) and (133), one obtains that

$$\langle Z\rangle(t_0) \notin I_S[\zeta_R(\tau_0)] \;\Rightarrow\; P(t_1) < \tfrac{1}{2}. \tag{134}$$

Hence, if an atom has probability $\geqslant 1/2$ of making the transition to the set of states (120) at the end of the π pulse, then its expected value of position $\langle Z\rangle(t_0) = \zeta(\tau_0)/\kappa$ is included in the interval $I_S[\zeta_R(\tau_0)]$ defined in (130).

Notice that the we never used the second factor in (122) with τ_1 given in (116) for the π pulse:

$$\sin^2\left\{\frac{\Omega_R[\zeta(\tau_0)]}{2}(\tau_1 - \tau_0)\right\} = \sin^2\left\{\frac{\pi\,\Omega_R[\zeta(\tau_0)]}{2\Omega_R[\zeta_R(\tau_0)]}\right\}. \tag{135}$$

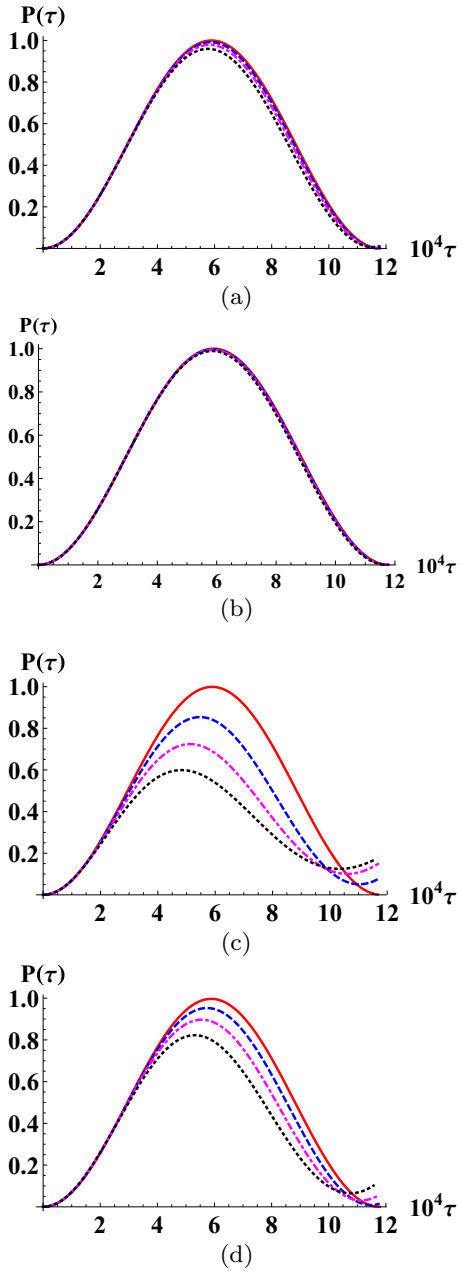

FIG. 2. (Color online) The figures show the probability $P(\tau)$ that the atom makes the transition for a 2π pulse as a function of the nondimensional time $\tau \in [\tau_0, \tau_1]$ for $B_0 = 0.3$ G and several values of the maximum height $\langle Z\rangle$ of the expected value of the position of the atom. The 2π pulse is applied from $\tau = \tau_0$ to $\tau = \tau_1$, with τ_0 the instant in which the atom reaches the maximum height $\langle Z\rangle$ starting from $z = 0$ at $t = 0$. The values are $\langle Z\rangle = 0$ cm (red solid lines), 0.4 cm (blue dashed lines), 1 cm (magenta dot-dashed lines), and 2 cm (black dotted lines). Panels (a) and (b) ((c) and (d)) have $\eta =$ 10 (100) G/cm. Also, panels (a) and (c) ((b) and (d)) have $\Delta Z(0) = 5 \times 10^{-7}$ (10^{-6}) m.

Therefore, the interval $I_{\min}[\zeta_R(\tau_0)]$ that satisfies

$$\langle Z\rangle(t_0) \in I_{\min}[\zeta_R(\tau_0)] \;\Leftrightarrow\; P(t_1) \geqslant \tfrac{1}{2} \tag{136}$$

is contained in $I_S[\zeta_R(\tau_0)]$ and has smaller length.

In the following we refer to *the atoms that have a probability* $\geqslant 1/2$ *of making the transition* as the *selected atoms*. Notice that we have taken the value $P(t_1) = 1/2$ to be the border between the atoms that made the transition and those that did not. We chose this value because we wanted to estimate the full width at half maximum (FWHM) of $P(t_1)$ as a function of the detuning between the transition angular frequency and the angular frequency ω_A of $\mathbf{B}_p(t)$. This detuning arises from the atoms not being located at the *resonant position* $\zeta_R(\tau_0)/\kappa$ [recall that ω_A was chosen so that the atoms make the transition with probability 1 if they are well localized around their expected value of position $\langle Z\rangle(t_0)$ at time t_0 and if $\langle Z\rangle(t_0) = \zeta_R(\tau_0)/\kappa$]. This is similar to the way in which the width of the selected velocities is calculated for Raman transitions [14] and to the way in which the *resonance width* of a sinusoidally varying perturbation of a time-independent Hamiltonian is calculated using perturbation theory [16].

The minimum value $\Delta_{z\mathrm{M}}$ of the length Δ_z of $I_S[\zeta_R(\tau_0)]$ is

$$\Delta_{z\mathrm{M}} = \lim_{x\to\pm\infty} \frac{4|\Omega_0(x)|}{\kappa\left|\frac{d}{dx}\left[V^0_{j_0}(x) - V^0_{j_1}(x)\right]\right|},$$
$$= \frac{1}{\left|\gamma_1 + F_-\gamma_2 + \frac{1}{2}\right|}\frac{B_0}{\eta}, \qquad (137)$$

The sign $\pm$ is chosen according to $j_0 = F_+, \pm F_+$. Notice that (137) establishes the best possible selection in terms of a simple functional relationship among the strength B_0 of the magnetic field $\mathbf{B}_p(t)$, the derivative η of $B_{\mathrm{ST}}(z)$, and a factor which depends on the alkali-metal atom used. On the other hand, the first line in (137) expresses $\Delta_{z\mathrm{M}}$ in terms of the (nondimensional) resonant Rabi frequency $\Omega_R[\zeta_R(\tau_0)] = 2|\Omega_0[\zeta_R(\tau_0)]|$ divided by the criterion (57) used to determine which transition gives place to the best phase-space selector. In fact, taking the limit in the denominator and evaluating the numerator at $x = \zeta_R(\tau_0)$ in the right side of the first line of (137) we obtain the following estimate involving the (angular) Rabi frequency $\Delta W\Omega_R[\zeta_R(\tau_0)]$ at the resonant position $\zeta_R(t_0)/\kappa$:

$$\Delta_{z\mathrm{M}} \simeq \frac{2}{\kappa\Delta W\left|\gamma_1 + F_-\gamma_2 + \frac{1}{2}\right|}\Delta W\Omega_R[\zeta_R(\tau_0)]. \qquad (138)$$

Therefore, the selection in position is better for smaller Rabi frequencies and larger values of η [recall that κ is proportional to η; see the definition in (29)].

We now use (130), (134), and (137) to characterize the selection in position and velocity described in the Introduction.

Assume that you have a cloud of noninteracting, well-localized, and identical alkali-metal atoms such that the expected value of the velocity of the cloud is zero. At time $t = 0$ prepare each atom in the state (72) with j_1 replacing j_0. At time $t = 0$ an arbitrary atom in the cloud has an expected value of position $z_0 = \zeta(0)/\kappa$ and an expected value of momentum p_0. Among all atoms in the cloud one wishes to select only those that are in a small neighborhood of $z_{0R} = \zeta_R(0)/\kappa$. Hence, one applies a π pulse with $t_0 = \tau_0/\Delta W = 0$. It follows from (134) that the selected atoms have z_0 in the interval $I_S(\kappa z_{0R})$.

Figure 3(a) shows a contour plot of the width Δ_z of $I_S(\kappa z_{0R})$ (units of m) for ^{87}Rb, $j_0 = F_+, F_+ = 2,2$, $j_1 = F_-, F_- = 1,1$, and $\eta = 100$ G/cm when $z_{0R} = \langle Z\rangle(t_0 = 0)$ is varied from 0 to 2 cm. We note that the change of Δ_z for the values of

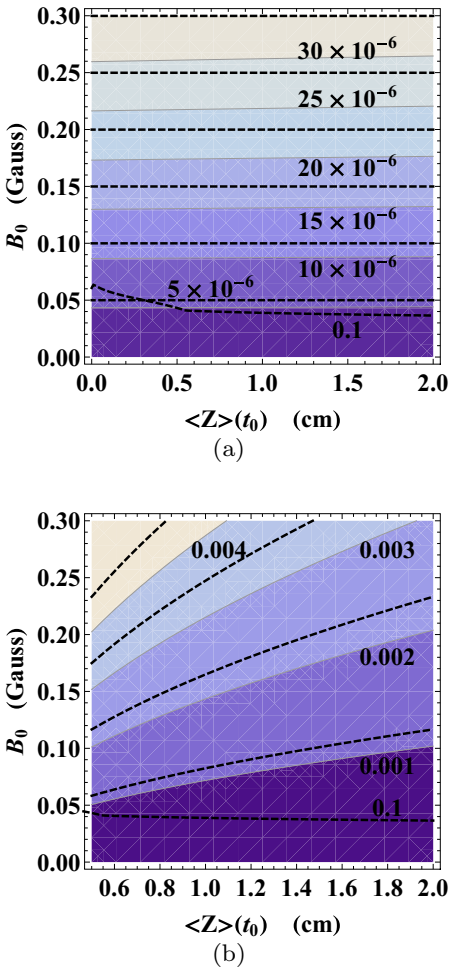

FIG. 3. (Color online) Panel (a) shows contour plots of the length Δ_z (purple solid lines) of the interval in (130) and of $\Delta_{z\mathrm{M}}$ (black dashed lines) as a function of $\zeta_R(\tau_0)/\kappa$ and B_0. The quantity $\zeta_R(\tau_0)/\kappa$ is denoted in the figure by $\langle Z\rangle(t_0)$. Panel (b) does the same for the width Δ_v (purple solid lines) of the velocity interval in (139) and for $\Delta_{v\mathrm{M}}$ (black dashed lines). The units of Δ_z and $\Delta_{z\mathrm{M}}$ are m, while those of Δ_v and $\Delta_{v\mathrm{M}}$ are m/s. Both figures have $\eta = 100$ G/cm and show the contour 0.1 (black dotted lines) above which the first-term approximation is accurate.

$\langle Z\rangle(t_0 = 0)$ considered is negligible (it is of order 5×10^{-7} m). Figure 3(a) also shows a contour plot (black dashed lines) of $\Delta_{z\mathrm{M}}$. The contours are exactly the same as those for Δ_z and appear displaced upwards. Observe that $\Delta_{z\mathrm{M}}$ gives a reasonable estimate of Δ_z for the lower values of B_0. We note that the first-term approximation is known to be accurate in the region above the contour 0.1 (black dotted line), since in that region the two-term approximation can correct the first-term approximation in at most 10%. The contour is exactly the same as that of Fig. 1(d). Finally, the duration $(t_1 - t_0)$ of the π pulse varies with $\langle Z\rangle(t_0 = 0)$, but is approximately equal to 1.36×10^{-6} s (40.8×10^{-6} s) for $B_0 = 0.3$ G ($B_0 = 0.01$ G) and the values of $\langle Z\rangle(t_0 = 0)$ shown.

If one wishes to make a selection in velocity, one proceeds as follows. At the end of the π pulse mentioned above we make a projective measurement to determine in which set of states $\{|z, V_j[x(z)]\rangle : z \in \mathbb{R}\}$ ($j = j_0 \mathrm{or} j_1$) each atom is found. Now

give *the cloud of selected atoms* (the cloud of atoms that did make the transition to the set of states $\{|z, V_{j_0}[x(z)]\rangle : z \in \mathbb{R}\}$) a *kick* upwards if $g_{\rm eff} > 0$ or downwards if $g_{\rm eff} < 0$. The new instant $t = 0$ corresponds to the end of the *kick*. The atoms in the selected cloud now have approximately the same initial expected values of position z_0 (the *kick* is brief), but new initial expected values of momentum $p_0 = \hbar\kappa\rho_0$. Since each of the atoms in the selected cloud is found in the set of states $\{|z, V_{j_0}[x(z)]\rangle : z \in \mathbb{R}\}$ and we are assuming that they are well localized, we approximate their initial states by (72).

Among all the atoms selected by the first pulse one wishes to select those with respective initial expected values of position and momentum z_{0R} and $p_{0R} = \hbar\kappa\rho_{0R}$. Apply a π pulse at the time $t_0 = \rho_{0R}/(q_2\Delta W) > 0$ [see (63) for the definition of q_2] when the atoms with expected value of position equal to $\zeta_R(\tau)/\kappa$ reach the maximum (minimum) height if $g_{\rm eff} > 0$ ($g_{\rm eff} < 0$). It follows that the selected atoms have their expected value of position $\langle Z\rangle(t_0)$ in the interval $I_S[\zeta_R(\tau_0)]$.

Each projective measurement can be performed by applying a laser that pushes away the atoms that did not make the transition. More precisely, one applies a laser that connects the set of states $\{|z, V_j[x(z)]\rangle : z \in \mathbb{R}\}$ (with $j = j_0$ or $j = j_1$ depending on which atoms one wants to push) with other states so as to have an optical transition. For example, in ^{87}Rb one could use the D_1 or D_2 lines [17]. The atoms that did not make the transition gain on average momentum in the direction of the traveling wave associated with the laser thanks to photons absorbed and subsequently emitted spontaneously. On the other hand, atoms that did make the transition are not pushed because they are far off resonance with the aforementioned optical transition.

The *kick* is also applied by using a laser that pushes (in the appropriate direction) the atoms that did make the transition and leaves them in the set of states $\{|z, V_{j_0}[x(z)]\rangle : z \in \mathbb{R}\}$. The duration of the application of the laser must be brief so that the momentum of the atoms is changed, leaving them at approximately the same position. In fact, the projective measurement mentioned above can be achieved directly with this *kick*.

Using that $\langle Z\rangle(0) \in I_S(\kappa z_{0R})$, $\langle Z\rangle(t_0) \in I_S[\zeta_R(\tau_0)]$, the forms of $\langle Z\rangle(t) = \zeta(\tau)/\kappa$ in (74) and of $\zeta_R(\tau)$ in (83), and that the second π pulse is applied when $\zeta_R(\tau)/\kappa$ reaches the maximum height [that is, $t_0 = \rho_{0R}/(q_2\Delta W)$ with q_2 defined in (63)], one can conclude that the atoms selected in the second π pulse have velocities $\langle P\rangle(t_0)/M$ in the interval

$$I_{2S}[\zeta_R(\tau_0)] = [l_{2-}[\zeta_R(\tau_0)], l_{2+}[\zeta_R(\tau_0)]], \tag{139}$$

with

$$l_{2\pm}[\zeta_R(\tau_0)] = \frac{1}{\kappa t_0}\{r_{\pm}[\zeta_R(\tau_0)] - r_{\mp}(\kappa z_{0R})\}. \tag{140}$$

Hence, a selection in velocity has been performed; that is, we have prepared a sample of atoms with well-defined velocity. Notice that, as a consequence of the second π pulse, the sample has also well-defined position.

Taking the limit $x \to \pm\infty$ according to $j_0 = F_+, \pm F_+$ we obtain the minimum length (width) of the velocity interval in (139),

$$\Delta_{v\rm M} = 2\frac{\Delta_{z\rm M}}{\Delta t}, \tag{141}$$

with Δt the time interval between pulses (in the case we are describing $\Delta t = t_0$). Hence, the best possible selection is again determined by a very simple formula which now includes the time Δt between pulses. Moreover, as time increases from $t = t_1$, the cloud of atoms in the set of states $\{|z, V_{j_0}[x(z)]\rangle : z \in \mathbb{R}\}$ becomes spatially separated from the cloud of atoms in the set of states $\{|z, V_{j_1}[x(z)]\rangle : z \in \mathbb{R}\}$, because the former moves under the potential $V_{j_0}[x(z)] + Mg_0z$, while the latter moves essentially under the different potential $V_{j_1}[x(z)] + Mg_0z$ [we say *essentially* because it moves under the potential $V_{j_1}[x(z)] + Mg_0z$ only if one neglects the weak coupling introduced by $\mathbb{L}^0(x)$; see (24) and (25)]. In other words, the clouds become separated due to the different response to the magnetic field of different Zeeman sublevels.

Figure 3(b) shows a contour plot of the length Δ_v of $I_{2S}[\zeta_R(\tau_0)]$ (units of m/s) for ^{87}Rb, $j_0 = F_+, F_+ = 2,2$, $j_1 = F_-, F_- = 1,1$, and $\eta = 100$ G/cm. The first pulse is applied for $z_{0R} = 0$. The maximum height $\zeta_R(t_0)/\kappa$ [denoted by $\langle Z\rangle(t_0)$ in the x axis of the figure] is varied from 0.5 to 2 cm. The figure also shows a contour plot of the minimum width $\Delta_{v\rm M}$ (black dashed lines) given in (141). The contours are exactly the same as those for Δ_v and appear displaced upwards. Notice that $\Delta_{v\rm M}$ estimates reasonably well Δ_v. As expected, Δ_v decreases for increasing maximum height [denoted by $\langle Z\rangle(t_0)$ in the figure], since the time between pulses is larger. Moreover, the first-term approximation is known to be accurate in the region above the contour 0.1 [this contour is exactly the same as the one in Fig. 1(d)]. We note that $a_0[\kappa\langle Z\rangle(t_0)] > 0$ for all values of $\langle Z\rangle(t_0)$ in the figure. Moreover, the duration $(t_1 - t_0)$ of the second π pulse is approximately the same as before.

A. Efficiency of the phase-space selector

We now discuss *how small* Δ_z and Δ_v really are. A cloud of ^{87}Rb atoms in a magneto-optical trap at a temperature $T = 20 \times 10^{-6}$ K can be modeled by Gaussian distributions f_r in position and f_v in velocity with respective standard deviations $\sigma_r \sim 10^{-3}$ m and $\sigma_v = \sqrt{k_B T/M} \sim 4.5 \times 10^{-2}$ m/s, with k_B the Boltzmann constant. Hence, the FWHM of f_r (f_v) is approximately equal to $2\sigma_r \sim 2 \times 10^{-3}$ m ($2\sigma_v \sim 10^{-1}$ m/s). From Figs. 3(a) and 3(b) it follows that the selection in position (velocity) can lead to a sample of atoms whose distribution in position (velocity) has a FWHM two orders of magnitude smaller.

Moreover, the recoil velocity of ^{87}Rb associated with the absorption or emission of a photon with wavelength λ_2 corresponding to the D_2 line [17] is $v_{\rm r}^{(2)} = 5.9 \times 10^{-3}$ m/s. From Fig. 3(b) one observes that f_v can have a FWHM of about $v_r/6 \simeq 0.001$ m/s if $B_0 \simeq 0.1$ G and $\eta = 100$ G/cm. Therefore, using the method we propose one may achieve a velocity resolution which tends to those obtained using velocity-dependent Raman transitions [3]. It is important to note that the widths of the selections in position and in velocity using our method are actually smaller than Δ_z and Δ_v, since we only know that the selected atoms have positions and velocities included in the intervals (130) and (139) [see (134) and (136)].

Velocity-dependent Raman transitions transfer atoms in a range of velocities of width [14]

$$\Delta v \simeq \frac{\lambda}{\Delta t_{\rm R}}, \tag{142}$$

where λ is the wavelength of the optical transition used in the Raman technique and Δt_{R} is the duration of the pulse. Note that the Raman technique uses a single long optical pulse whose duration appears in the denominator in (142), while the proposed method uses two short microwave pulses separated by Δt in (141). Hence, the proposed method relaxes the experimental requirements for frequency stability when compared to the Raman technique.

Finally, we discuss what happens when the atom is not well localized around its expected value of position $\langle Z\rangle(t_0) = \zeta(\tau_0)/\kappa$ at time $t_0 = \tau_0/\Delta W$ for a fixed B_0. In this case it was observed in Sec. VD that the probability that the atom makes the transition decreases considerably when its expected value of position is equal to the resonant position $\zeta_R(\tau_0)/\kappa$. Hence, the phase-space selector does not work since atoms that should make the transition, in fact, do not. In Sec. VD it was also shown that increasing B_0 increases the probability that the atom makes the transition and that the atom can be considered to be well localized for sufficiently large values of B_0. Hence, if the atom is not well localized for a given value of B_0 one must then increase B_0 until the atom can be considered to be well localized. Once this is done all the results established in Sec. VI apply. It is important to note that by increasing B_0 one is not localizing the atom, one is simply making the interaction of the atom with $\mathbf{B}_p(t)$ less sensitive to the position of the atom. For example, assume that $\Delta Z(0) = 10^{-6}$ m and that $\eta = 100$ G/cm. From Fig. 1(d) it follows that B_0 must take a value between 0.3 and 0.5 G in order to have a probability of making the transition approximately equal to 1 when $\zeta_R(\tau_0)/\kappa$ [denoted by $\langle Z\rangle(t_0)$ in the figure] varies from 0 to 2 cm. For these values of B_0 the atom can be considered to be well localized and the results of Sec. VI can be applied. From Fig. 3(b) it then follows that the length Δ_v of the interval in (139) is $\Delta_v \simeq 0.003, 0.005$ m, which is still quite good. In conclusion, in order to apply the results of Sec. VI one must use values of B_0 that are compatible with the condition of having a well-localized atom and these values of B_0 are determined by demanding that the atoms with expected value of position equal to the resonant position $\zeta_R(\tau_0)/\kappa$ have probability of making the transition approximately equal to 1. It is important to note that the expansion of the center-of-mass wave packet is the principal phenomenon limiting the efficiency of the proposed phase-space selector, since it affects the values of B_0 that can be used. If a way is found to limit the expansion, then smaller widths can be obtained.

VII. CONCLUSIONS

In this article we established a model that describes any alkali-metal atom interacting with a position- and time-dependent classical magnetic field. It includes the hyperfine structure of the atom and quantizes its center-of-mass motion. Moreover, we proposed a method directed to prepare samples of atoms with both well-defined position and well-defined velocity. The method is based on magnetic dipole transitions between hyperfine levels whose energy separation depends on the position of the atoms due to the presence of a position-dependent static magnetic field such as the one found in a magneto-optical trap.

The model was used to characterize the proposed method. It was determined which transitions give place to the best selections in position and velocity and the evolution of the state of the atom was calculated analytically. Simple expressions where obtained for relevant physical quantities such as the probability that the atom makes a transition, the expected values of position, momentum, and energy, and their dispersions. This allowed us to calculate approximately the widths of the selected positions and velocities and to establish the efficiency of the method. It was concluded that the proposed method can lead to samples of atoms whose width in velocity tends to those obtained using velocity-dependent Raman transitions. Also, it was concluded that the main phenomenon prohibiting smaller widths in position and velocity is the expansion of the atomic center-of-mass wave packet. If a way can be found to circumvent this problem, then much smaller widths are possible.

It is important to note that the idea on which the proposed method is based consists of taking a cloud of atoms and applying magnetic pulses that are resonant with a previously defined transition only for atoms located at a certain position. The dependence on position of the energy separations of the levels of the atoms is achieved by using a static magnetic field that depends on position, while a time-dependent magnetic field (the pulse) is used to make transitions between the levels. One pulse selects those atoms that are located around a certain position, while a second pulse separated by a time interval from the first one selects the atoms at another position. The effect of the two pulses is to select from the cloud of atoms a sample with both well-defined position and well-defined velocity. Although the method was analyzed only for alkali metals, it could be applied for other types of atoms. Moreover, we considered the case where the second pulse is applied when the atoms that want to be selected reach a maximum height. The reason for this is that the first-term approximation used to characterize the widths of the selections in position and velocity is accurate in this case. Nevertheless, the second pulse could be applied during the flight of the cloud of atoms. The analytic expressions for the widths are still valid if the first-term approximation is accurate, but this accuracy would have to be checked using, for example, the criterion presented in the article.

The proposed method is specially attractive because it is easier to implement experimentally than velocity-dependent Raman transitions and can lead to comparable results. Moreover, it has the advantage that it also selects in position. Hence, it also offers an alternative to the use of slits and holes in plates to perform this task. Finally, we mention that it might be possible to combine the proposed method with the Raman technique to prepare samples of atoms with both well-defined velocity and well-defined position.

ACKNOWLEDGMENTS

The authors want to thank CONACYT and the Universidad Nacional Autónoma de México for support. We also thank Victor M. Valenzuela from the Universidad Autónoma de Sinaloa for fruitful discussions.

APPENDIX A

In this appendix we review a model used to describe the internal structure of an alkali-metal atom of mass M. We consider the nucleus and the electrons of the full shells as a single-point particle of mass $M - m_e$ (m_e is the mass of the electron), spin I equal to the spin of the nucleus, and position equal to the position of the nucleus. In the following we refer to this particle as the *core particle* and we assume it is fixed at the coordinate origin. Moreover, we also assume that $I \geqslant 1/2$. The core particle acts as a center of force that affects the valence electron which is referred to simply as the electron.

The state space of the atom is

$$\mathcal{H} = \mathcal{H}_{er} \otimes \mathcal{H}_{es} \otimes \mathcal{H}_{I}, \tag{A1}$$

where $\mathcal{H}_{er}$ and $\mathcal{H}_{es}$ are the state spaces for the spatial and spin degrees of freedom of the electron, respectively, and $\mathcal{H}_{I}$ is the state space for the spin degrees of freedom of the core particle.

The Hamiltonian of the atom is [13,14]

$$H_A = H_e + H_{\mathrm{SO}} + H_{\mathrm{HFS}}, \tag{A2}$$

where H_e is the sum of the kinetic and potential energies of the electron

$$H_e = \frac{1}{2m_e}\mathbf{P}_e^2 + V(R_e), \tag{A3}$$

H_{SO} is the spin-orbit interaction of the electron

$$H_{\mathrm{SO}} = \xi(R_e)\mathbf{L}\cdot\mathbf{S}, \tag{A4}$$

and H_{HFS} is the hyperfine Hamiltonian. An explicit expression for H_{HFS} is given later.

Here $\mathbf{R}_e$, $\mathbf{P}_e$, $\mathbf{S}$, and $\mathbf{L} = \mathbf{R}_e \times \mathbf{P}_e$ are respectively the position, momentum, spin, and orbital angular momentum operators of the electron, while $V(r)$ is a spherically symmetric non-Coulomb potential and

$$\xi(r) = \frac{1}{2m_e^2c^2}\frac{1}{r}\frac{dV}{dr}(r), \tag{A5}$$

with c the speed of light in vacuum.

Now the goal is to define the ground-state configuration of the atom and to introduce an orthonormal basis for it. In order to do this we first diagonalize H_e in $\mathcal{H}_{er}$.

Since H_e commutes with the three components of $\mathbf{L}$, one can diagonalize simultaneously H_e, $\mathbf{L}^2$, and L_z in $\mathcal{H}_{er}$. Hence, there exists an orthonormal basis

$$\begin{aligned}\beta_{er} = \{&|n,l,m_l\rangle : n = n_0, n_0+1, \ldots,\\ &-l \leqslant m_l \leqslant l,\ l = 0,1,\ldots,n-1\},\end{aligned} \tag{A6}$$

for $\mathcal{H}_{er}$ composed of eigenvectors of H_e, $\mathbf{L}^2$, and L_z, that is,

$$\begin{aligned} H_e|n,l,m_l\rangle &= E_{n,l}|n,l,m_l\rangle,\\ \mathbf{L}^2|n,l,m_l\rangle &= l(l+1)\hbar^2|n,l,m_l\rangle,\\ L_z|n,l,m_l\rangle &= m_l\hbar|n,l,m_l\rangle.\end{aligned} \tag{A7}$$

We remark that β_{er} is a standard basis; that is, the action of the angular momentum ladder operators $L_\pm$ on its elements satisfy the usual relations [16].

In the following we consider only the ground-state configuration of the atom; that is, we restrict to the following subspace of $\mathcal{H}$,

$$\mathcal{H}_0 \equiv \mathcal{H}_{er}^0 \otimes \mathcal{H}_{es} \otimes \mathcal{H}_{I}, \tag{A8}$$

with $\mathcal{H}_{er}^0$ the subspace of $\mathcal{H}_{er}$ spanned by the basis

$$\{|k_0\rangle \equiv |n_0,l = 0,m_l = 0\rangle\}. \tag{A9}$$

Notice that our use of the model of a single electron interacting with a core particle to describe an alkali-metal atom is entirely adequate because we are restricting the principal quantum number n to its lowest possible value n_0.

Now everything is set to introduce a basis for $\mathcal{H}_0$. Since $\mathcal{H}_{es}$ and $\mathcal{H}_{I}$ are the state spaces for the spin degrees of freedom of the electron and of the core particle, respectively, we can choose standard bases

$$\begin{aligned}\beta_{es} &= \{|s = 1/2,m_s\rangle : m_s = \pm 1/2\},\\ \beta_{I} &= \{|I,m_I\rangle : m_I = I, I-1,\ldots,-I\},\end{aligned} \tag{A10}$$

for $\mathcal{H}_{es}$ and $\mathcal{H}_{I}$ composed of eigenvectors of $\mathbf{S}^2$, S_z, $\mathbf{I}^2$, and I_z; that is,

$$\begin{aligned} \mathbf{S}^2|s = 1/2,m_s\rangle &= \tfrac{3}{4}\hbar^2|s = 1/2,m_s\rangle,\\ S_z|s = 1/2,m_s\rangle &= m_s\hbar|s = 1/2,m_s\rangle,\\ \mathbf{I}^2|I,m_I\rangle &= I(I+1)\hbar^2|I,m_I\rangle,\\ I_z|I,m_I\rangle &= m_I\hbar|I,m_I\rangle.\end{aligned} \tag{A11}$$

Here $\mathbf{I}$ is the spin angular momentum operator of the nucleus (or core particle).

From (A8)–(A11) it follows that β_0 in (2) is an orthonormal basis for $\mathcal{H}_0$ composed of eigenvectors of H_e, $\mathbf{L}^2$, L_z, $\mathbf{S}^2$, S_z, $\mathbf{I}^2$, and I_z. Notice that the dimension of $\mathcal{H}_0$ is $\dim\mathcal{H}_0 = 2(2I+1)$. Also,

$$\begin{aligned}\beta_{\mathrm{esI}} = \{&|m_s,m_I\rangle \equiv |s = 1/2,m_s\rangle \otimes |I,m_I\rangle :\\ &m_s = \pm 1/2, m_I = I, I-1,\ldots,-I\},\end{aligned} \tag{A12}$$

is an orthonormal basis for $\mathcal{H}_{es} \otimes \mathcal{H}_{I}$ composed of eigenvectors of $\mathbf{S}^2$, S_z, $\mathbf{I}^2$, and I_z.

Now we proceed to diagonalize H_A in $\mathcal{H}_0$. Notice that for this to make sense it must result that $\mathcal{H}_0$ is an invariant subspace under H_A.

From (A7)–(A9) first observe that

$$\mathbf{L} = 0, \quad H_e + H_{\mathrm{SO}} = E_{n_0,0} \quad \text{in} \quad \mathcal{H}_0. \tag{A13}$$

Using this result in (A2) it follows that to diagonalize H_A in $\mathcal{H}_0$ we only need to diagonalize H_{HFS}. It can be shown [14,16] that the restriction of H_{HFS} to $\mathcal{H}_0$ takes the form

$$H_{\mathrm{HFS}} = \frac{a}{\hbar^2}\mathbf{I}\cdot\mathbf{J} \quad \text{in} \quad \mathcal{H}_0, \tag{A14}$$

where $a > 0$ is a constant, $\mathbf{J} = \mathbf{L} + \mathbf{S}$ is the total angular momentum of the electron.

Introducing the total angular momentum of the atom $\mathbf{F} = \mathbf{J} + \mathbf{I}$, we can express H_{HFS} in the form

$$H_{\mathrm{HFS}} = \frac{a}{2\hbar^2}(\mathbf{F}^2 - \mathbf{J}^2 - \mathbf{I}^2) \quad \text{in} \quad \mathcal{H}_0. \tag{A15}$$

Therefore, to diagonalize H_{HFS} in $\mathcal{H}_0$ we need to diagonalize simultaneously $\mathbf{F}^2$, $\mathbf{J}^2$, and $\mathbf{I}^2$ in $\mathcal{H}_0$.

Using (A13) it follows that

$$\mathbf{J} = \mathbf{S}, \quad \mathbf{F} = \mathbf{S} + \mathbf{I} \quad \text{in} \quad \mathcal{H}_0, \tag{A16}$$

and it is clear that $\mathbf{S}^2$, $\mathbf{I}^2$, $\mathbf{F}^2$, and F_z can be diagonalized simultaneously in $\mathcal{H}_{es} \otimes \mathcal{H}_I$. Hence, there exists a standard basis

$$\beta_{\text{esI}}^{\text{C}} = \{|F, M_F\rangle : -F \leqslant M_F \leqslant F,\ F = I \pm 1/2\}, \tag{A17}$$

for $\mathcal{H}_{es} \otimes \mathcal{H}_I$ composed of eigenvectors of $\mathbf{S}^2$, $\mathbf{I}^2$, $\mathbf{F}^2$, and F_z; that is,

$$\begin{aligned} \mathbf{S}^2|F, M_F\rangle &= \tfrac{3}{4}\hbar^2|F, M_F\rangle, \\ \mathbf{I}^2|F, M_F\rangle &= I(I+1)\hbar^2|F, M_F\rangle, \\ \mathbf{F}^2|F, M_F\rangle &= F(F+1)\hbar^2|F, M_F\rangle, \\ F_z|F, M_F\rangle &= M_F\hbar|F, M_F\rangle. \end{aligned} \tag{A18}$$

Using $\beta_{\text{esI}}^{\text{C}}$ one can define the orthonormal basis β_0^{C} for $\mathcal{H}_0$ given in (3) and (4) composed of eigenvectors of H_e, $\mathbf{L}^2$, L_z, $\mathbf{S}^2$, $\mathbf{I}^2$, $\mathbf{F}^2$, and F_z.

Using (A2), (A13), (A15), (A16), and (A18) it follows that

$$\begin{aligned} H_A|k_0, F, M_F\rangle = &\left\{E_{n_0,0} + \frac{a}{2}\left[F(F+1) - I(I+1) - \frac{3}{4}\right]\right\} \\ &\times |k_0, F, M_F\rangle, \end{aligned} \tag{A19}$$

for $M_F = -F, \ldots, F$ and $F = I \pm 1/2$. Hence, β_0^{C} in (3) is an orthonormal basis for $\mathcal{H}_0$ composed of eigenvectors of H_A and $\mathcal{H}_0$ is an invariant subspace under H_A.

All the information about the hyperfine structure of the ground-state configuration of the atom is contained in (3) and (A19). We find that the ground-state configuration of the atom has two possible energies (eigenvalues of H_A):

$$E_+ \equiv E_{n_0,0} + \frac{a}{2}I, \quad E_- \equiv E_{n_0,0} - \frac{a}{2}(I+1). \tag{A20}$$

The energy E_+ is $(2I+2)$ degenerate, while E_- is $2I$ degenerate. Moreover, the vectors $|k_0, F = F_+, M_F\rangle$ ($M_F = F_+, F_+ - 1, \ldots, -F_+$) have energy E_+, while the kets $|k_0, F = F_-, M_F\rangle$ ($M_F = F_-, F_- - 1, \ldots, -F_-$) have energy E_-. To simplify the notation we have used the quantities in (4). Finally, we note that the field-free ground-state (energy) hyperfine splitting is

$$\hbar\Delta W \equiv E_+ - E_- = \frac{a}{2}(2I+1). \tag{A21}$$

Introduction of a classical magnetic field

We now introduce a constant classical magnetic field along the z axis $\mathbf{B} = B\mathbf{z}$ with $B \in \mathbb{R}$. The Hamiltonian of the system atom + magnetic field is given in (6) and (7). We note that the state space of the system is still given by $\mathcal{H}$ in (A1). What is not immediately clear is if it still makes sense to restrict to the subspace $\mathcal{H}_0$. This happens if and only if $\mathcal{H}_0$ is invariant under $-\boldsymbol{\mu}\cdot\mathbf{B}$. From (A11) and (A13) we find that

$$-\boldsymbol{\mu}\cdot\mathbf{B}|k_0, m_s, m_I\rangle = \hbar B\left(g_s\frac{\mu_B}{\hbar}m_s - g_I\frac{\mu_N}{\hbar}m_I\right)|k_0, m_s, m_I\rangle. \tag{A22}$$

Hence, β_0 is an orthonormal basis for $\mathcal{H}_0$ composed of eigenvectors of $-\boldsymbol{\mu}\cdot\mathbf{B}$ and $\mathcal{H}_0$ is invariant under H_{AB}.

We now proceed to diagonalize H_{AB} in $\mathcal{H}_0$. Given the definitions of H_A in (A2) and H_{AB} in (6), it follows from (A13) that this is accomplished if we diagonalize $H_{\text{HFS}} - \boldsymbol{\mu}\cdot\mathbf{B}$. Since F and M_F are no longer good quantum numbers, the basis β_0^{C} is not useful and we return to the basis β_0 in (2). First, define the sets

$$\begin{aligned} \beta(M_F) = \{&|k_0, m_s = 1/2, m_I = M_F - 1/2\rangle, \\ &|k_0, m_s = -1/2, m_I = M_F + 1/2\rangle\}, \\ \beta(M_F = \pm F_+) = \{&|k_0, m_s = \pm 1/2, m_I = \pm I\rangle\}, \end{aligned} \tag{A23}$$

for $M_F = F_-, F_- - 1, \ldots, -F_-$ [recall the definition of $F_\pm$ in (4)]. It is clear that

$$\beta_0 = \bigcup_{M_F=-F_+}^{F_+} \beta(M_F). \tag{A24}$$

Moreover, using (A15), (A16), (A22), and the electron and nuclear spin angular momentum ladder operators $S_\pm$ and $I_\pm$ it is straightforward to show that $\beta(M_F)$ spans a subspace of $\mathcal{H}_0$, denoted by $\text{span}\beta(M_F)$, that is invariant under H_{HFS}, $-\boldsymbol{\mu}\cdot\mathbf{B}$, and F_z for each $M_F = F_+, F_+ - 1, \ldots, -F_+$. In particular, the matrix representation of $H_{\text{HFS}} - \boldsymbol{\mu}\cdot\mathbf{B}$ in $\text{span}\beta(M_F)$ is

$$[H_{\text{HFS}} - \boldsymbol{\mu}\cdot\mathbf{B}]_{\beta(M_F)} = \frac{\hbar\Delta W}{2I+1}\begin{pmatrix} M_F - \frac{1}{2} & \sqrt{I(I+1) - M_F^2 + \frac{1}{4}} \\ \sqrt{I(I+1) - M_F^2 + \frac{1}{4}} & -\left(M_F + \frac{1}{2}\right) \end{pmatrix} + \frac{\hbar B}{2}\begin{pmatrix} U_+ & 0 \\ 0 & U_- \end{pmatrix}, \tag{A25}$$

with

$$U_\pm = \pm g_s\frac{\mu_B}{\hbar} - 2g_I\left(M_F \mp \frac{1}{2}\right)\frac{\mu_N}{\hbar}, \tag{A26}$$

for each $-F_- \leqslant M_F \leqslant F_-$. These are 2×2 matrices and can be diagonalized easily [16]. Using (A13) it follows that the eigenvectors of each of these matrices along with the vectors in $\beta(M_F = \pm F_+)$ define the orthonormal basis $\Gamma(x)$ in (8) and (9) composed of eigenvectors of H_{AB}. Explicitly, one has

$$H_{\text{AB}}\left|V_{F,M_F}(x)\right\rangle = \left[E_{n_0,0} - \frac{\hbar\Delta W}{2(2I+1)} + V_{F,M_F}(x)\right]\left|V_{F,M_F}(x)\right\rangle, \tag{A27}$$

for each $-F \leqslant M_F \leqslant F$ and $F = F_\pm$. Moreover, it is easy to show that

$$\begin{aligned}\mathbf{F}^2|V_{F_+,\pm F_+}(x)\rangle &= F_+(F_+ + 1)\hbar^2|V_{F_+,\pm F_+}(x)\rangle,\\ \mathbf{F}^2\big|V_{F,M_F}(x)\big\rangle\big|_{B=0} &= F(F+1)\hbar^2\big|V_{F,M_F}(x)\big\rangle\big|_{B=0},\end{aligned} \tag{A28}$$

for each $-F_- \leqslant M_F \leqslant F_-$, $F = F_\pm$.

To simplify the formula in (A27) we now redefine the zero of the energy scale in such a way that

$$E_{n_0,0} - \frac{\hbar\Delta W}{2(2I+1)} \to 0. \tag{A29}$$

This can be accomplished by redefining H_A to be

$$H_A = H_e + H_{\mathrm{SO}} + H_{\mathrm{HFS}} - \left[E_{n_0,0} - \frac{\hbar\Delta W}{2(2I+1)}\right], \tag{A30}$$

which reduces to (1) when restricted to $\mathcal{H}_0$. In particular, with (A30) the formulas (5) and (10) are satisfied.

APPENDIX B

Consider a pair of parallel circular coils of radius R carrying steady currents in opposite directions. Establish a coordinate system such that one of the coils carries a current $I_c > 0$ and has its center at $(0,0,d_0)$ with $d_0 > 0$, while the other coil carries a current $-I_c$ and has its center at $(0,0,-d_0)$. We now establish several approximations for the magnetic field $\mathbf{B}_{2\mathrm{C}}(\mathbf{r})$ produced by the two coils.

Using the Biot-Savart law and the Taylor series expansion of $(1+x)^{-3/2}$ with center at $x = 0$, it follows that

$$\mathbf{B}_{2\mathrm{C}}(\mathbf{r}) \sim B_{\mathrm{ST}}(z)\mathbf{z}, \tag{B1}$$

to zero order in x/R and y/R with

$$B_{\mathrm{ST}}(z) = \frac{\mu_0 I_c}{2}\left\{\frac{R^2}{[R^2+(z-d_0)^2]^{3/2}} - \frac{R^2}{[R^2+(z+d_0)^2]^{3/2}}\right\}. \tag{B2}$$

$B_{\mathrm{ST}}(z)\mathbf{z}$ will be an accurate approximation of $\mathbf{B}_{2\mathrm{C}}(\mathbf{r})$ if

$$\frac{3}{4}\left(\frac{\sqrt{x^2+y^2}}{R}\right) \ll 1. \tag{B3}$$

This condition was obtained by asking that terms linear in x/R and y/R be much smaller than (B2).

It is important to notice that $B_{\mathrm{ST}}(z)\mathbf{z}$ does not satisfy the Maxwell equation $\boldsymbol{\nabla}\cdot\mathbf{B} = 0$. Nevertheless, it does constitute an accurate approximation to $\mathbf{B}_{2\mathrm{C}}(\mathbf{r})$ if the condition in (B3) is fulfilled. To obtain an approximation that does satisfy $\boldsymbol{\nabla}\cdot\mathbf{B} = 0$, the expansion has to be carried to order $(2n-1)$ in x/R and y/R $(n = 1,2,\ldots)$.

Again, using the Biot-Savart law and the Taylor series expansion of $(1+x)^{-3/2}$ with center at $x = 0$ it follows that

$$B_{2\mathrm{C}}(\mathbf{r}) \sim \alpha_1\frac{z}{\sqrt{R^2+d_0^2}}\mathbf{z} + \alpha_2(z)\left(\frac{x}{R}\mathbf{x} + \frac{y}{R}\mathbf{y}\right), \tag{B4}$$

to order 1 in x/R, y/R, and $z/\sqrt{R^2+d_0^2}$, with

$$\begin{aligned}\alpha_2(z) &= \frac{3\mu_0 I_c}{4}\frac{R^2}{\left(R^2+d_0^2\right)^{3/2}}\\ &\quad\times\left[\frac{\frac{z-d_0}{R}}{1+\left(\frac{z-d_0}{R}\right)^2} - \frac{\frac{z+d_0}{R}}{1+\left(\frac{z+d_0}{R}\right)^2}\right],\\ \alpha_1 &= 3\mu_0 I_c\frac{R^2 d_0}{\left(R^2+d_0^2\right)^2}.\end{aligned} \tag{B5}$$

The expression on the right of (B4) will be an accurate approximation of $B_{2\mathrm{C}}(\mathbf{r})$ if the following conditions are satisfied:

$$|z \pm d_0| \gg 2\sqrt{x^2+y^2}, \quad 2|z| \ll d_0. \tag{B6}$$

These conditions were obtained by asking that the first correction to (B4) be much smaller than (B4).

If in addition to (B6), the condition

$$\sqrt{x^2+y^2} \ll |z|\frac{4d_0/R}{1+(d_0/R)^2} \tag{B7}$$

is satisfied, then the term multiplied by $\alpha_2(z)$ in (B4) can be dropped out and an accurate approximation to $B_{2\mathrm{C}}(\mathbf{r})$ is given by

$$B_{2\mathrm{C}}(\mathbf{r}) \sim \eta z\mathbf{z}, \tag{B8}$$

with

$$\eta = \mu_0 I_c\frac{3R^2 d_0}{\left(R^2+d_0^2\right)^{5/2}}. \tag{B9}$$

For example, taking $d_0 = R$, it follows from (B4)–(B9) that $\eta z\mathbf{z}$ is an accurate approximation of $B_{2\mathrm{C}}(\mathbf{r})$ if the following conditions hold:

$$2\sqrt{x^2+y^2}, \quad 2|z| \ll R, \quad \frac{1}{2}\sqrt{x^2+y^2} \ll |z|. \tag{B10}$$

In summary, the magnetic field produced by the two coils is approximately equal to $\eta z\mathbf{z}$ if one is sufficiently close to the axis of the coils, sufficiently far away from the origin, and sufficiently far away from the coils.

APPENDIX C

In this appendix we extend the model of Appendix A to include the quantized center-of-mass motion of the alkali-metal atom.

Now consider that the core particle is no longer fixed at the coordinate origin. It has position and momentum operators $\mathbf{R}$ and $\mathbf{P}$, respectively, and the atom is subject to a constant gravitational field. In Appendix A the position of the electron was measured from the coordinate origin which was the position of the core particle (and of the nucleus). Now the position of the electron is measured from the position of the core particle (which coincides with the position of the nucleus), $\mathbf{R}_e$ is the associated operator, and $\mathbf{P}_e$ is the corresponding conjugate momentum.

The state space of the atom is now

$$\mathcal{H}_T = \mathcal{H}_{\text{core}} \otimes \mathcal{H}, \tag{C1}$$

where $\mathcal{H}_{\text{core}}$ is the state space for the spatial degrees of freedom of the core particle and $\mathcal{H}$ is given in (A1).

The Hamiltonian that describes an alkali-metal atom subject to a constant gravitational field is now

$$H_{AT} = \frac{1}{2(M-m_e)}\mathbf{P}^2 + (M-m_e)g_0 Z + m_e g_0 (Z+Z_e) + H_A, \tag{C2}$$

where $g_0 = 9.8\ \text{m/s}^2$ is the acceleration of gravity and H_A is given in (A30). Notice that H_{AT} is the sum of the kinetic energy of the core particle, plus the gravitational potential energies of the core particle and the electron, plus the Hamiltonian H_A describing the internal degrees of freedom of the alkali-metal atom. We can simplify (C2) as follows:

$$H_{AT} = \frac{1}{2M(1-m_e/M)}\mathbf{P}^2 + Mg_0\left(Z + \frac{m_e}{M}Z_e\right) + H_A. \tag{C3}$$

Now we neglect the terms multiplied by m_e/M in (C3) to obtain the Hamiltonian

$$H_{AT} = \frac{1}{2M}\mathbf{P}^2 + Mg_0 Z + H_A. \tag{C4}$$

Notice that by neglecting the terms multiplied by m_e/M we are identifying the position of the core particle (which coincides with the position of the nucleus) with the position of center of mass of the atom. Therefore, we refer to the core particle also as the center-of-mass particle when this approximation is used. Since $m_e/M \ll 1$ and the expected value $\langle Z_e\rangle(t)$ of Z_e at any time t satisfies $|\langle Z_e\rangle(t)| \sim a_0$ with a_0 the Bohr radius, the approximation works well. Moreover, it gets progressively better as heavier alkali-metal atoms are considered. For example, $m_e/M = 5.4\times10^{-4}$ for hydrogen, while $m_e/M = 6.3\times10^{-6}$ for ^{87}Rb.

The ground-state configuration of the atom now corresponds to the subspace $\mathcal{H}_{\text{CM}} \otimes \mathcal{H}_0$, where we define $\mathcal{H}_{\text{CM}} = \mathcal{H}_{\text{core}}$ and $\mathcal{H}_0$ is still defined by (A8). All the results about $\mathcal{H}_0$ obtained in Appendix A are valid.

1. Introduction of a classical magnetic field

We now introduce a classical magnetic field $\mathbf{B}(\mathbf{r},t)$. The state space of the system [alkali-metal atom with quantized center-of-mass motion subject to a constant gravitational field and interacting with $\mathbf{B}(\mathbf{r},t)$] is still given by (C1), while the ground-state configuration is still given by $\mathcal{H}_{\text{cm}} \otimes \mathcal{H}_0 = \mathcal{H}_{\text{core}} \otimes \mathcal{H}_0$.

The Hamiltonian of the system is

$$H_{3D}(t) = H_{AT} - \left(-g_l\frac{\mu_B}{\hbar}\mathbf{L} - g_s\frac{\mu_B}{\hbar}\mathbf{S}\right)\cdot\mathbf{B}(\mathbf{R}+\mathbf{R}_e,t) - g_l\frac{\mu_N}{\hbar}\mathbf{I}\cdot\mathbf{B}(\mathbf{R},t), \tag{C5}$$

where H_{AT} is given in (C4) and the rest of the terms on the right are described in Appendix A.

We now assume that $\mathbf{B}(\mathbf{r},t)$ varies with respect to $\mathbf{r}$ on a scale much larger than the average distance of the electron to the core particle. Then one can make the long-wavelength approximation in (C5) to obtain the following Hamiltonian:

$$H_{3D}(t) = \frac{1}{2M}\mathbf{P}^2 + Mg_0 Z + H_A - \boldsymbol{\mu}\cdot\mathbf{B}(\mathbf{R},t). \tag{C6}$$

We emphasize that (C6) was obtained using the long-wavelength approximation and neglecting terms multiplied by m_e/M.

2. Reduction to one dimension

Now assume that

$$\mathbf{B}(\mathbf{r},t) = \mathbf{B}_{2C}(\mathbf{r}) + \mathbf{B}_p(\mathbf{r},t), \tag{C7}$$

where $\mathbf{B}_{2C}(\mathbf{r})$ is the magnetic field of Appendix B and

$$\mathbf{B}_p(\mathbf{r},t) = B_0\mathbf{b}_p\text{Re}\{e^{i[kx-\omega_A(t-t_0)]}\}, \tag{C8}$$

with $\mathbf{r} = (x,y,z)$, $B_0 > 0$, $\mathbf{b}_p$ a constant real unit vector perpendicular to the x axis, $k = \omega_A/c$, and Re the real part of a complex number.

Assume that for all time of interest t one has $k|\langle X\rangle(t)| \ll 1$ and the condition (B3) in Appendix B is satisfied for $x = \langle X\rangle(t)$, $y = \langle Y\rangle(t)$, and $z = \langle Z\rangle(t)$. Here $\langle X\rangle(t)$, $\langle Y\rangle(t)$, and $\langle Z\rangle(t)$ are the expected values of the position of the atom in the x, y, and z directions at time t. From the results of Appendix B and from (C8) it follows that accurate approximations of $\mathbf{B}_{2C}(\mathbf{r})$ and $\mathbf{B}_p(\mathbf{r},t)$ are

$$\mathbf{B}_{2C}(\mathbf{r}) \sim B_{ST}(z)\mathbf{z}, \qquad \mathbf{B}_p(\mathbf{r},t) \sim \mathbf{B}_p(t) = B_0\mathbf{b}_p\text{Re}[e^{-i\omega_A(t-t_0)}], \tag{C9}$$

with $B_{ST}(z)$ in (B2). If in addition conditions (B6) and (B7) in Appendix B are satisfied for all time of interest t and for $x = \langle X\rangle(t)$, $y = \langle Y\rangle(t)$, and $z = \langle Z\rangle(t)$, then $B_{ST}(z)$ can be approximated by ηz with η in (B9).

Using the approximations (C9) in (C6) one obtains

$$H_{3D}(t) = \left(\frac{1}{2M}P_x^2 + \frac{1}{2M}P_y^2\right) + H(t), \tag{C10}$$

with $H(t)$ given in (11). Therefore, $H_{3D}(t)$ is separable. The center-of-mass motion of the atom in the xy plane corresponds to that of a free particle moving in two dimensions, while the center-of-mass motion along the z axis and the internal degrees of freedom of the atom evolve according to the Hamiltonian $H(t)$ studied in the article.

APPENDIX D

In this appendix we prove (26); that is, we prove that $[\mathcal{L}_{jk}(z)]^\dagger = \mathcal{L}_{kj}(z)$ [see (25) for the definition of $\mathbb{L}(z)$].

Assume that $\phi(z),\psi(z) \in S(\mathbb{R})$ and that $1 \leqslant j,k \leqslant \dim\mathcal{H}_0 = 2(2I+1)$. Recall that $f(z) \in S(\mathbb{R})$ if and only if $f(z)$ is an infinitely differentiable complex-valued function defined on $\mathbb{R}$ such that the product of any polynomial times any derivative of $f(z)$ [including the zero derivative, that is, $f(z)$] tends to zero if $x \to \pm\infty$ [22].

In what follows we use the more succinct notation

$$\sum_{F,M_F}(\cdot) \equiv \sum_{F=F_\pm}\sum_{M_F=-F}^{F}(\cdot). \tag{D1}$$

Also, from (3) we have the completeness relationship

$$\sum_{F,M_F} |k_0,F,M_F\rangle\langle k_0,F,M_F| = \mathbb{I}_0, \tag{D2}$$

where $\mathbb{I}_0$ is the identity operator in $\mathcal{H}_0$.

Substituting the definition of $\mathcal{L}_{jk}(z)$ given in (22), adding and subtracting the operator $\partial^2/\partial z^2$ inside the curly brackets in the expression of $\mathcal{L}_{jk}(z)$ in (22), and grouping the terms associated with the second partial derivative of $\langle k_0,F,M_F|V_k[x(z)]\rangle\psi(z)$ with respect to z, one obtains that

$$\begin{aligned}
&\int_{-\infty}^{+\infty} dz\phi(z)^*[\mathcal{L}_{jk}(z)\psi(z)] \\
&\quad = \sum_{F,M_F}\left(-\frac{\hbar^2}{2M}\right)\int_{-\infty}^{+\infty} dz\phi(z)^*\langle V_j[x(z)]|k_0,F,M_F\rangle \\
&\qquad \times\left\{\frac{\partial^2}{\partial z^2}\langle k_0,F,M_F|V_k[x(z)]\rangle\psi(z)\right. \\
&\qquad \left. -\langle k_0,F,M_F|V_k[x(z)]\rangle\frac{\partial^2}{\partial z^2}\psi(z)\right\}.
\end{aligned} \tag{D3}$$

Now integrate by parts the first term inside the curly brackets in (D3) and note that the resulting boundary terms are zero because $\phi(z),\psi(z)\in S(\mathbb{R})$. Also, use (D2) to simplify the integral associated with the the second term inside the curly brackets in (D3). Then one obtains that

$$\begin{aligned}
&\int_{-\infty}^{+\infty} dz\phi(z)^*[\mathcal{L}_{jk}(z)\psi(z)] \\
&\quad = \sum_{F,M_F}\left(-\frac{\hbar^2}{2M}\right)\int_{-\infty}^{+\infty} dz\langle k_0,F,M_F|V_k[x(z)]\rangle\psi(z) \\
&\qquad \times\frac{\partial^2}{\partial z^2}\phi(z)^*\langle V_j[x(z)]|k_0,F,M_F\rangle \\
&\qquad +\frac{\hbar^2}{2M}\int_{-\infty}^{+\infty} dz\phi(z)^*\langle V_j[x(z)]|V_k[x(z)]\rangle\frac{\partial^2}{\partial z^2}\psi(z).
\end{aligned} \tag{D4}$$

Expanding the second-order partial derivative in the first integral in (D4), using the definition of $\mathcal{L}_{kj}(z)$ in (22), and using (D2) to simplify the resulting integrals, it follows that

$$\begin{aligned}
&\int_{-\infty}^{+\infty} dz\phi(z)^*[\mathcal{L}_{jk}(z)\psi(z)] \\
&\quad = \int_{-\infty}^{+\infty} dz[\mathcal{L}_{kj}(z)\phi(z)]^*\psi(z) \\
&\qquad -\frac{\hbar^2}{2M}\int_{-\infty}^{+\infty} dz\psi(z)\langle V_j[x(z)]|V_k[x(z)]\rangle\frac{\partial^2}{\partial z^2}\phi(z)^* \\
&\qquad +\frac{\hbar^2}{2M}\int_{-\infty}^{+\infty} dz\phi(z)^*\langle V_j[x(z)]|V_k[x(z)]\rangle\frac{\partial^2}{\partial z^2}\psi(z).
\end{aligned} \tag{D5}$$

Using $\langle V_j[x(z)]|V_k[x(z)]\rangle = \delta_{jk}$ [see (9)], integrating by parts the last integral in (D5) and noting that boundary terms are zero because $\phi(z),\psi(z)\in S(\mathbb{R})$, it follows from (D5) that

$$\begin{aligned}
&\int_{-\infty}^{+\infty} dz\phi(z)^*[\mathcal{L}_{jk}(z)\psi(z)] \\
&\quad = \int_{-\infty}^{+\infty} dz[\mathcal{L}_{kj}(z)\phi(z)]^*\psi(z).
\end{aligned} \tag{D6}$$

Using the definition of the adjoint of an operator one concludes from (D6) that

$$[\mathcal{L}_{jk}(z)]^\dagger = \mathcal{L}_{kj}(z). \tag{D7}$$

[1] M. Kasevich, D. S. Weiss, E. Riis, K. Moler, S. Kasapi, and S. Chu, Phys. Rev. Lett. **66**, 2297 (1991).

[2] K. Moler, D. S. Weiss, M. Kasevich, and S. Chu, Phys. Rev. A **45**, 342 (1992).

[3] J. Chabé, H. Lignier, P. Szriftgiser, and J. C. Garreau, Opt. Commun. **274**, 254 (2007).

[4] M. Kasevich and S. Chu, Phys. Rev. Lett. **67**, 181 (1991).

[5] M. Kasevich and S. Chu, Appl. Phys. B **54**, 321 (1992).

[6] T. L. Gustavson, P. Bouyer, and M. A. Kasevich, Phys. Rev. Lett. **78**, 2046 (1997).

[7] M. L. Terraciano, S. E. Olson, M. Bashkansky, Z. Dutton, and F. K. Fatemi, Phys. Rev. A **76**, 053421 (2007).

[8] J. Stuhler, M. Fattori, T. Petelski, and G. M. Tino, J. Opt. B **5**, S75 (2003).

[9] R. Battesti, P. Cladé, S. Guellati-Khélifa, C. Schwob, B. Grémaud, F. Nez, L. Julien, and F. Biraben, Phys. Rev. Lett. **92**, 253001 (2004).

[10] M. Ben Dahan, E. Peik, J. Reichel, Y. Castin, and C. Salomon, Phys. Rev. Lett. **76**, 4508 (1996).

[11] J. Ringot, P. Szriftgiser, J. C. Garreau, and D. Delande, Phys. Rev. Lett. **85**, 2741 (2000).

[12] D. A. Steck, W. H. Oskay, and M. G. Raizen, Phys. Rev. Lett. **88**, 120406 (2002).

[13] L. I. Schiff, *Quantum Mechanics*, 3rd ed. (McGraw-Hill, New York, 1968).

[14] C. J. Foot, *Atomic Physics* (Oxford University Press, Oxford, UK, 2005).

[15] M. Tinkham, *Group Theory and Quantum Mechanics* (Dover, New York, 2003).

[16] C. Cohen-Tannoudji, B. Diu, and F. Laloë, *Quantum Mechanics* (Wiley, New York, 1977), Vols. I and II.

[17] D. A. Steck, Rubidium 87 D Line Data, Los Alamos National Laboratory, 2003.

[18] G. Breit and I. Rabi, Phys. Rev. **38**, 2082 (1931).

[19] C. F. Bunge, J. A. Barrientos, and A. V. Bunge, At. Data Nucl. Data Tables **53**, 113 (1993).

[20] http://www.astro.umd.edu/~miller/nstar.html.

[21] A. Messiah, *Quantum Mechanics* (Dover, New York, 2008).

[22] W. Rudin, *Functional Analysis*, 2nd ed. (McGraw-Hill, New York, 1991).
[23] E. Zauderer, *Partial Differential Equations of Applied Mathematics*, 3rd ed. (Wiley, New York, 2006).
[24] L. O. Castaños and R. Jáuregui, Phys. Rev. A **82**, 053815 (2010).
[25] E. A. Coddington and R. Carlson, *Linear Ordinary Differential Equations* (SIAM, Philadelphia, 1997).
[26] C. Cohen-Tannoudji, J. Dupont-Roc, and G. Grynberg, *Atom-Photon Interactions* (Wiley, New York, 1998).